Sustainable Cities and Society 128 (2025) 106437

Contents lists available at ScienceDirect

Sustainable Cities and Society

journal homepage: www.elsevier.com/locate/scs

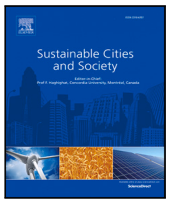

Enhancing flood resilience of urban rail transit systems through recovery resource scheduling optimisation: A case study of London

Wei Bi [a,b,*], Jürgen Hackl [c], Kristen MacAskill [a,b]

[a] Centre for Sustainable Development, Department of Engineering, University of Cambridge, Cambridge CB2 1PZ, United Kingdom
[b] Centre for Smart Infrastructure and Construction, Department of Engineering, University of Cambridge, Cambridge CB3 0FA, United Kingdom
[c] Department of Civil and Environmental Engineering, Princeton University, Princeton, NJ, 08544, United States

ARTICLE INFO

Keywords:
Urban rail transit systems
Flood resilience
Recovery resource scheduling
Genetic algorithm
Network modelling
Climate change adaptation

ABSTRACT

As heavy rainfall increasingly disrupts services of urban rail transit systems (URTSs), enhancing their resilience to flood risks is crucial to sustaining reliable public transport, particularly amid growing climate challenges. To investigate the effectiveness of potential interventions for mitigating post-flood impacts on URTS operations, this research introduces a novel application of genetic algorithms to optimise recovery resource scheduling for URTSs following large-scale flood-induced disruptions. The objective is to reduce economic impacts related to revenue loss and operational impacts concerning disruptions to passenger travel. By systematically integrating network topology, operational performance, flood disruption scenarios, and recovery profiles, the methodology is demonstrated through the London URTS under 30-year, 100-year, and 1,000-year flood risk scenarios. Compared to a topological attribute-determined benchmark, the optimised resource scheduling solutions have a tangible effect in reducing post-flood impacts. In the London case study, revenue loss can be reduced by 10.9%, 10.7%, and 6.7% across the respective flood scenarios, corresponding to savings of approximately £337K, £708K, and £760K, along with decreased unmet travel demand of 197K, 404K and 470K. These results demonstrate the significance of strategic resource scheduling in ensuring effective recovery from large-scale flood disruptions, offering valuable insights for disaster risk management, especially for extreme weather scenarios.

1. Introduction

Urban rail transit systems (URTSs) – such as metros, light rail, and trams – are critical infrastructure that provides reliable, affordable, and accessible passenger service for all communities around urban and suburban areas. In recent years, however, their capacity to fulfil this role has been challenged by increasingly heavy rainfall and storm events, which often result in widespread flash floods (IPCC, 2023b). These extreme events often occur with little warning and can rapidly develop into fast-flowing water (UK Met Office, 2019; US NOAA, 2016), submerging at-grade tracks or invading underground platforms and tunnels through openings such as station entrances. Flooding incidents affecting URTSs have occurred in cities such as New York City (Matthew, 2021), London (JBA, 2021), Zhengzhou (Gan & Wang, 2021), Hong Kong (Mok et al., 2023), Milan (Browning, 2023), and Madrid (Reyes, 2023), where extensive service disruptions, severe economic loss, consequential social impacts, and even passenger fatalities were observed. Given these circumstances, the concept of resilience has received considerable attention as a means to cope with extreme weather events, emphasising a system's ability to withstand, recover from, and adapt to disruptions (The White House, 2013).

Pathways for enhancing the resilience of transport systems can be characterised into ex-ante risk mitigation and ex-post response and recovery. As presented in Fig. 1, ex-ante mitigation measures aim to reduce the immediate impacts resulting from failures, such as casualties, instant loss of services, and equipment damage. To achieve this, the most widely applied strategy is enhancing system robustness by upgrading physical infrastructure, ensuring the system continues to function without disproportionate degradation (strategy R1). In the practice of URTS flood resilience, specific actions include hardening pumping systems, adding additional steps to station entrances, or installing flood gates at station entrances (Metropolitan Transportation Authority, 2024). Another strategy is to build permanent redundancy into the system to moderate impacts by providing alternative pathways to maintain services (strategy R2). In the context of URTS flood resilience, actions include building new metro lines to strengthen connectivity (e.g., the London Elizabeth Line Transport for London, 2024a) or developing alternative drainage systems to channel floodwater. However,

* Correspondence to: Department of Engineering, University of Cambridge, Cambridge, CB2 1PZ, United Kingdom.
E-mail address: wb316@cam.ac.uk (W. Bi).

https://doi.org/10.1016/j.scs.2025.106437
Received 2 December 2024; Received in revised form 3 April 2025; Accepted 7 May 2025
Available online 22 May 2025

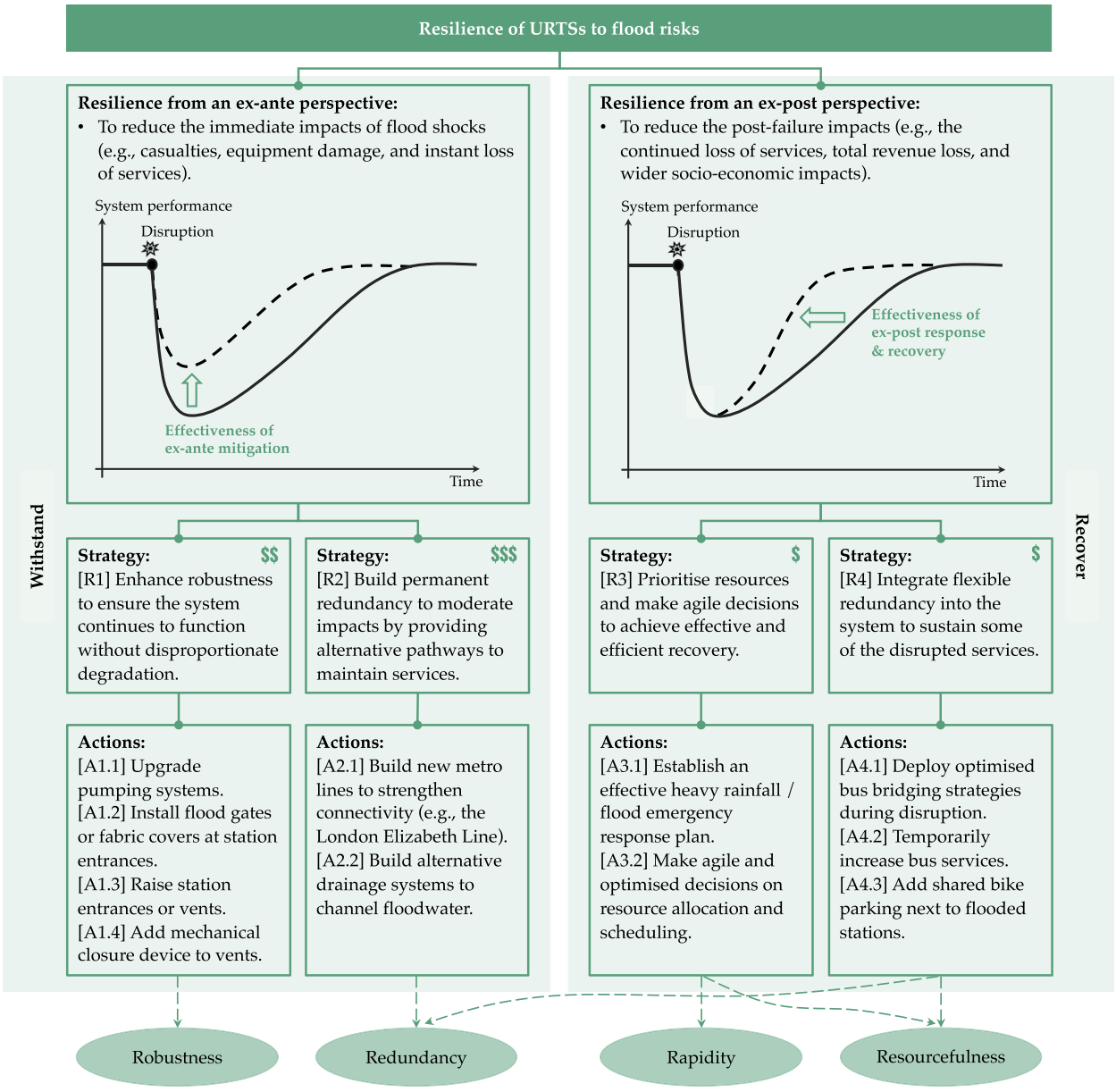

Fig. 1. Pathways for enhancing URTS flood resilience.

the feasibility of implementing this strategy can be limited by factors such as budget constraints, available technologies, and urban planning considerations.

While ex-ante mitigation measures represent the current dominant approach in practice (as observed such as in Maryland Transit Administration, 2023; Metropolitan Transportation Authority, 2024, and Transport for London (2023a)) and are fundamental for managing recurrent and credible risks, they often fall short against extreme but plausible adverse conditions. An illustrative example is the repeated flooding incidents within the New York City Subway, despite $7.6 billion capital investment in repair, upgrades, and additional protection following Hurricane Sandy in 2012 (Metropolitan Transportation Authority, 2024). In this case, ex-post response and recovery measures show great promise, emphasising the significance of minimising post-failure impacts (Serdar et al., 2022), such as continued loss of services, total revenue loss, and wider socio-economic impacts. This aspect of resilience, distinctive from other safety management principles, highlights the essence of resilience—effective recovery following disruptions (Linkov et al., 2014). Strategies in this regard include, first and foremost, prioritising resources and making agile decisions to achieve effective and efficient recovery (strategy R3) (Zhang et al., 2022; Zheng et al., 2023), including actions such as establishing a flood emergency response plan and optimising the scheduling of limited resources. Another strategy is to integrate flexible redundancy into the system to sustain some of the disrupted services (strategy R4). These actions are normally ad hoc and, in the practice of URTS flood resilience, could include arranging bus bridging to sustain URTS services (Itani & Shalaby, 2021; Jin et al., 2016; Zhang, Ren, & Song, 2023), increasing bus services to accommodate passengers displaced from suspended rail transit routes (Jin et al., 2014; Liu, Chen, et al., 2022; Xu, Lu, et al., 2024), or deploying shared bike parking next to flooded stations (Metropolitan Transportation Authority, 2024).

This study adopts the less emphasised recovery perspective, focusing specifically on optimising critical resource scheduling within strategy R3, for four primary reasons. Firstly, IPCC (2023a) projections suggest

that the impacts of climate change, including more frequent and intensive floods, are likely to increase until at least 2050 and potentially beyond 2100. In this case, flood-induced service disruptions of URTSs are likely to become more frequent and severe, making effective recovery increasingly crucial. Secondly, although strategy R4 are beneficial in sustaining services during disruptions, they do not directly contribute to the effective restoration of a URTS itself. Thirdly, post-flood recovery is a complex process that necessitates resources – such as emergency crews and pumps – that are often limited in supply. When multiple system elements are flooded simultaneously, the scheduling of these resources plays a critical role in affecting recovery efficiency and the overall impacts of service disruptions. However, research into examining the effectiveness of a URTS's recovery from large-scale yet plausible flood disruptions has received scant attention (discussed further in Section 2). Lastly, resource scheduling in practical recovery operations is predominantly experience-based, relying on practitioners' existing knowledge of operational criticality of stations under normal conditions. However, these factors can shift significantly during disruptions as the network topology and system dynamics evolve. Transit agencies often lack the capacity to reassess station criticality at a system level during disruptions and lack tools to optimise resource scheduling in the case of widespread disruptions caused by extreme floods. This further underscores the importance of this study.

Hence, to bridge the research gap, this study aims to demonstrate the value of optimising recovery resource scheduling in minimising post-flood impacts of URTS service disruptions, thereby enhancing URTS flood resilience through effective recovery. Building on an advanced URTS flood resilience assessment model developed from the authors' recent work (Bi et al., 2024), this research introduces a novel application of genetic algorithms (GAs) to optimise resource scheduling solutions. The primary objective is to minimise total revenue loss during flood disruptions, as this is an important and meaningful financial concern for transit agencies (Transport for London, 2023a). The effectiveness in reducing unsatisfied travel demand is also examined to evaluate reduced impacts on passenger travel. This approach is demonstrated through a case study on 15 lines of the London URTSs under 30-year, 100-year, and 1,000-year flood disruption scenarios. This study has contributed to the field of disaster risk management of complex infrastructure systems in following ways:

(a) This study marks the first step towards demonstrating the critical role of effective restoration of URTSs following large-scale service disruptions under extreme flood risk scenarios, highlighting its value as a potentially cost-effective strategy for disaster risk management. While constructing a system that can withstand a 1,000-year flood event is often impractical and cost-prohibitive, this study provides a viable approach to building up capacity to scenario-test how to recover effectively. This costs little compared to undertaking construction works and can equip operators to familiarise themselves with critical sections within the system and manage recovery in an informed way.
(b) The modelling methodology integrates a significant level of system complexity and dynamics to deliver a holistic view of URTS disruptions and recovery, accounting for a rail transit network model, origin–destination travel demand in the millions, system-level service disruption simulations in the context of flooding, recovery options and their applicability, recovery times, emergency crew scheduling optimisation for post-flood impact mitigation, and assessments of direct economic consequences and disrupted journeys (i.e., operational performance loss) throughout disruption periods. The advancements in integrated dynamic modelling for simulating extreme scenarios, quantifying impacts, and optimising recovery contribute to the growing body of knowledge on resilience-centred climate change adaptation for complex infrastructure systems, particularly in light of the current emphasis on ex-ante risk mitigation by enhancing system robustness (Ouyang et al., 2019). Such modelling advancements also lay the foundational building blocks for developing digital twins tailored to crisis management in URTSs.
(c) In comparison with existing literature that only analyses a system segment (Goldbeck et al., 2019), this study showcases the approach through a real-world large-scale URTS that exhibits complex system dynamics and thereby enhances its practical relevance. The proposed framework can be flexibly applied to enhance the flood resilience of other networked infrastructure systems, such as roads, railways, or power grids, by quantifying meaningful performance indicators, stress-testing the system with varying scenarios, and exploring alternative optimisation objectives (e.g., minimising social impacts).
(d) This study closely aligns with the UN Sustainable Development Goals 9 (build resilient transport infrastructure), 11 (invest in public transport for sustainable cities), and 13 (climate action) (United Nations, 2015): developing flood resilient URTSs is a cornerstone that supports socio-economic activities in urban and suburban areas, and optimising resource scheduling during flood disruptions contributes to the rapid recovery of service delivery. This not only aids in reinforcing urban sustainability and the flood resilience of URTSs but also advances the broader objective of establishing enduring and trustworthy public transport services.

The remainder of this paper is outlined as follows. Section 2 provides a literature review of methods employed to determine or optimise recovery resource scheduling for enhancing infrastructure resilience. Section 3 introduces the methodology designed to optimise the scheduling of emergency crews during recovery following flood disruptions in URTSs. Section 4 describes the London case study. The results are detailed in Section 5, followed by a discussion in Section 6. The conclusions and contributions are summarised in Section 7.

2. Literature review

2.1. Review methodology

Optimising recovery resource scheduling has been a subject of recent studies for networked infrastructure systems such as transport, power grids, or water distribution networks, as the inherent dependencies between system elements change dynamically during recovery and can remarkably affect system performance. To examine how this topic is addressed specifically in the context of recovering URTSs from large-scale flooding under extreme weather scenarios, a literature investigation is conducted by applying the query string for searching in the title, abstract, and keywords: TS = ((flood OR flooding OR rain* OR storm OR (weather AND event) OR (extreme AND weather)) AND (metro OR subway OR (rail AND transit) OR (rapid AND transit)) AND (recover* OR restor* OR repair)) in the Web of Science and Scopus. A total of 115 English publications, including articles, conference papers, reviews, books, and book chapters, were initially obtained after removing duplicates. However, upon reviewing titles, keywords, and abstracts, none of these studies was specifically designed to address this question. This absence presents the potential for contributions in this field.

The subsequent section reviews how this topic has been addressed within the broader scope of infrastructure systems, regardless of the causes of disruptions, to provide a reference for developing the methodology in this study. A broader query string for searching in the title, TI = ((infrastructure OR transport* OR road OR rail OR transit OR metro OR subway OR air* OR water OR power OR community) AND (recover* OR restor* OR repair) AND (resilien*)), was applied in the Web of Science and Scopus, yielding 394 publications after removing duplicates. After reviewing titles, keywords, and abstracts, 80 publications were identified as relevant. Fig. 2 presents a statistical overview of these

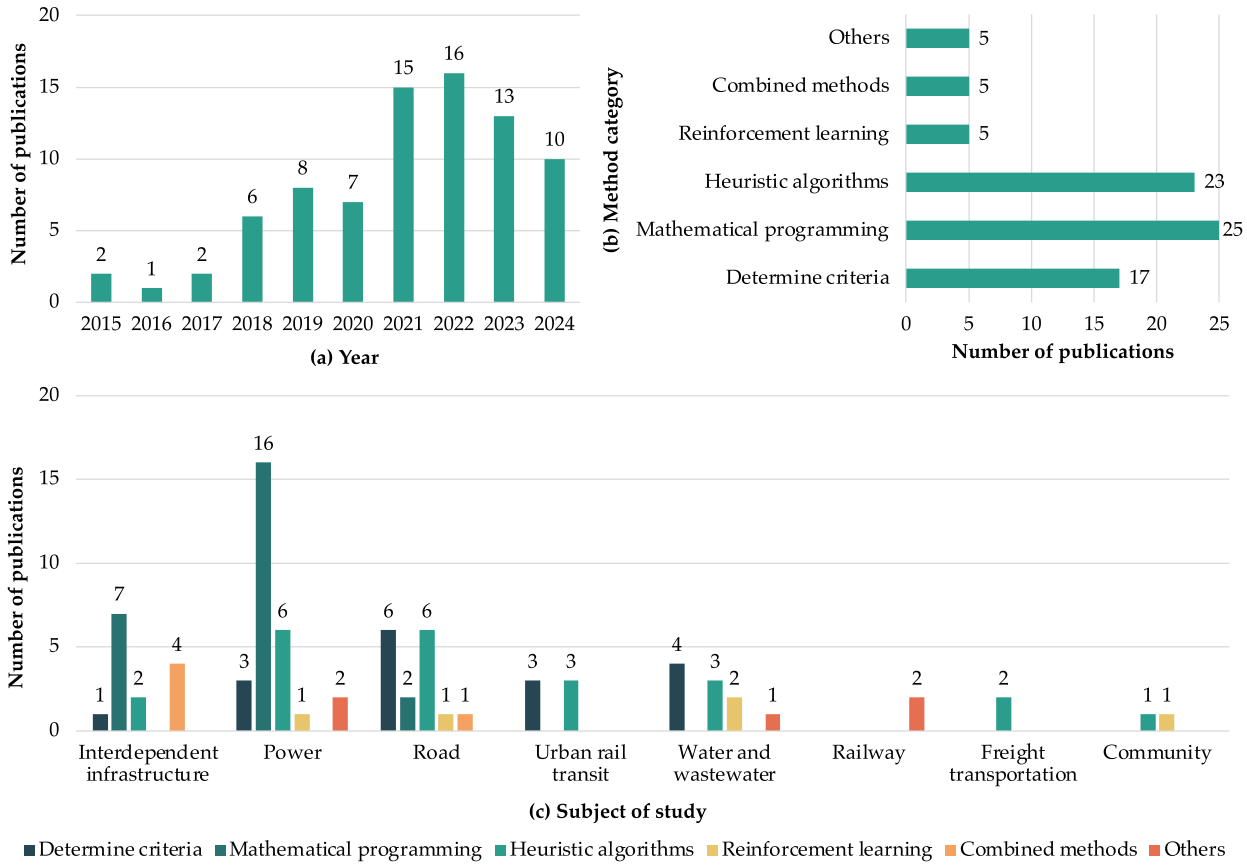

Fig. 2. Publications for optimising recovery resource scheduling by (a) year, (b) method category, and (c) subject of study (as of 27 May 2024).

publications categorised by year, method, and subject of study. The overview indicates a generally rising trend in the study of this topic, covering multiple critical infrastructure systems and four principal categories of methods: determining criteria, mathematical programming, heuristic algorithms, and reinforcement learning.

2.2. Methods for determining or optimising recovery resource scheduling

2.2.1. Determining criteria

The first group of studies uses deterministic criteria for establishing recovery sequences, primarily focusing on importance-based strategies. These importance indicators include topological attributes (Beyza et al., 2020; Li et al., 2023; Serdar & Al-Ghamdi, 2023; Xu & Xu, 2024) and integrated metrics such as performance (Merschman et al., 2020; Wu et al., 2021; Yang et al., 2018), vulnerability (Saadat et al., 2020), and network robustness (Liu, McNeil, et al., 2022). Other criteria are developed based on repair time (Du et al., 2023; Figueroa-Candia et al., 2018) or distance (Liu et al., 2020; Yang et al., 2018). While adopting these criteria is straightforward and applicable across a variety of infrastructure systems, they may not yield optimal or near-optimal results and lack the capacity for thorough investigation.

2.2.2. Mathematical programming

To address this limitation, scholars utilise mathematical programming to find an optimal resource scheduling sequence. Stochastic programming (Fang & Sansavini, 2019; Kong et al., 2023; Xu, Li, & Chen, 2024) or mixed integer programming (Almoghathawi et al., 2019, 2021; Arab et al., 2015; Arjomandi-Nezhad et al., 2020; Aziz et al., 2023; Edib et al., 2023; Karakoc et al., 2019; Lei et al., 2019; Li et al., 2021; Luo & Yang, 2021; Mao et al., 2021; Sadnan et al., 2022; Sang et al., 2021) are usually applied. These approaches are primarily utilised for studying power systems (see Fig. 2(c)). They work well for problems that can be accurately modelled using mathematical formulations. However, the computational complexity can increase exponentially with the size and dimension of the problem, making mathematical programming less feasible for very large or complex problems. Taking the 30-year flood disruption scenario of the London URTS developed by Bi et al. (2024) as an example, 125 stations and tracks are identified flooded, with each having one to three applicable recovery options – pump, manual, or natural recovery – depending on their flood depths and locations. In the case where each flooded element has two applicable recovery options, the size of the resource scheduling solution space would be $125! \times 2^{125}$ (approximately 8.01×10^{246}). Even considering a localised historical flooding event on 12 July 2021 in London, where 34 stations were recorded flooded, the size of the solution space would still be large, calculated as $34! \times 2^{34}$ (approximately 5.07×10^{48}), which is generally not feasible for implementing mathematical programming.

2.2.3. Reinforcement learning

Furthermore, with the rapid development of artificial intelligence, reinforcement learning has begun to show promise in finding near-optimal recovery resource scheduling solutions for systems like roads (Fan et al., 2023), power grids (Wang et al., 2023), water distribution networks (Fan et al., 2022), and small-scale interdependent infrastructure within a university campus (Yang et al., 2024). By treating the scheduling problem as a Markov Decision Process, reinforcement learning aims to train an agent to make sequential decisions towards achieving a specific goal by learning from trial-and-error interactions with a simulated environment (Sutton & Barto, 2018). Although this approach offers a novel way to navigate system dynamics and complexity, its effectiveness can be tempered by the need for extensive hyperparameter tuning (e.g., learning rate, discount factor, entropy coefficient, size of the hidden layer of neural networks), which requires

Table 1
Case studies in relevant reinforcement learning studies and this paper.

Research	Network size of the case study	Disruption scenario and size
Fan et al. (2022)	Water distribution network in Fairfield, California: 112 nodes and 126 pipes	Simulated M6.5 earthquake: affecting 44 pipes (only edge failures)
Fan et al. (2023)	Road network in University Heights, Cleveland: 95 junctions and 141 road segments	Simulated flooding: affecting 16–34 road segments in varying scenarios (only edge failures)
Wang et al. (2023)	IEEE 33-bus power network: 8 essential loads, 15 non-essential loads, 6 photovoltaic generation, 3 diesel generators, and 5 MESS stations	Random outage scenarios generated through the Monte Carlo sampling technique: affecting of around 11 lines (only edge failures)
Yang et al. (2024)	Tsinghua University campus: 82 pipelines, 3 wells, 1 main substation, 12 distribution substations, and 5 bridges	Simulated M8 earthquake: affecting 47 pipelines, 2 wells, 12 substations, and 5 bridges (both node and edge failures)
This paper	15 lines of the London URTS: 443 stations and 533 tracks	30-year flood: affecting 44 stations and 81 tracks; 100-year flood: affecting 82 stations and 146 tracks; 1,000-year flood: affecting 149 stations and 228 tracks (both node and edge failures)

substantial computational resources to identify satisfactory settings for specific problems. Additionally, compared to the network sizes of the testbeds in these four studies listed in Table 1, the London URTS and its flood disruption scenarios examined in this research is much larger in scale, presenting increased challenges in implementing this approach.

2.2.4. Heuristic algorithms

An alternative approach for achieving near-optimal scheduling solutions in complex recovery operations is heuristic algorithms. These algorithms include simulated annealing algorithms (Hackl et al., 2018; Liu, Chen, et al., 2022; Wu et al., 2020), greedy search algorithm (Li et al., 2018), tabu search algorithm (Wang et al., 2019), ant colony algorithm (Cheng & Zhang, 2022), and particle swarm optimisation algorithms (Moghtadernejad et al., 2022), with GAs being the most widely applied due to their flexibility and efficiency. GAs emulate the essential features of natural selection and have been applied to optimise recovery resource scheduling in general disruption contexts for road (Liu et al., 2021; Mao et al., 2021; Pan et al., 2022; Somy et al., 2022; Zhang et al., 2017), urban rail transit (Zhang et al., 2022; Zheng et al., 2023; Zhu et al., 2021), water distribution networks (Assad et al., 2020; Han et al., 2020; Song et al., 2022), and interdependent infrastructure systems (Kong et al., 2019; Liu et al., 2024; Pei et al., 2024; Xu, Li, & Chen, 2024; Zhang et al., 2024, 2018). The algorithm starts with generating an initial population that represents a set of potential solutions to the optimisation problem, followed by selecting individuals (i.e., solutions) for reproduction based on their fitness values. This process mirrors natural selection, where more adaptive individuals are more likely to mate and transmit their advantageous traits (Endler, 1986). Subsequently, these selected individuals reproduce to create offspring that form a new generation through crossover and mutation. These processes introduce variability into the population, analogous to genetic diversity in biological organisms. This new population replaces the old population and repeats the above procedure until a satisfactory solution is found or a predetermined number of generations is reached. The best solution in the final generation is considered as the final output.

In rail transit applications, Zheng et al. (2023) employ a GA to optimise the recovery sequence of metro stations under random, intentional, and range failure scenarios, aiming at maximising a normalised resilience index that integrates network global efficiency and unaffected traffic. Regarding the range failure scenarios, they identify three flood-prone points in the studied city, which yield ten flooded stations out of a total of 164. Results show that the GA-derived solution performs better than other criticality-based recovery sequences generated based on metrics such as node degree or network efficiency. Recovery details such as repair time and resource constraints are not introduced in this study. Zhang et al. (2022) take into account budget limitation and repair time uncertainty in their analysis, applying a Non-dominated Sorting Genetic Algorithm II (NSGA-II) to optimise restoration sequence of damaged metro stations. The objective is to maximise the network global efficiency. The study examines two scenarios generated based on historical natural disasters (though details unspecified) in which 20 stations experienced damage. Repair times are randomly assigned using a distribution function. Zhu et al. (2021) also employ the NSGA-II to determine station repair sequence, considering constraints on repair resource and repair capacity. The algorithm aims to minimise performance loss, which is indicated by the proportion of unaffected passengers. Only random and targeted failure scenarios are studied.

While these three studies have demonstrated the suitability of GAs for optimising the recovery sequences of metro stations, they are not sufficiently equipped to simulate the recovery of URTSs from large-scale disruptions caused by extreme flooding, nor do they focus on evaluating URTS resilience with practically meaningful performance indicators. To be specific, employing network global efficiency as the performance indicator captures system resilience solely from the physical connectivity perspective, offering limited insights for understanding flood impacts of URTS service disruptions (Bi et al., 2023). Moreover, the scales of disruptions examined in these studies are small. More importantly, while widely applied random failure scenarios are often adopted to represent natural hazards and technical failures, and targeted failure scenarios typically depict terrorist attacks, both are overly abstract for capturing flood-induced disruptions. This is because the extent of flood impacts varies according to geographical, topographical, hydrological, and engineering factors of infrastructure assets, resulting in disruptions that are neither purely random nor entirely targeted. Additionally, detailed recovery profiles, which account for the methods and resources specifically required for recovery from floods, are absent in these studies. In light of the above, this study further investigates the potential of GAs through a novel application aimed at optimising recovery resource scheduling to enhance the resilience of URTSs to extreme flood risks, incorporating detailed recovery profiles, meaningful resilience indicators, and plausible flood risk scenarios. GAs are selected as they are recognised for their ability to effectively handle large search spaces due to their robust global search capacities (Lambora et al., 2019).

3. Methodology

This section illustrates how this study adopts GAs to optimise recovery resource scheduling for URTSs during extreme floods and introduces benchmark solutions for evaluating optimisation performance. Prior to this, Section 3.1 provides an overview of the URTS flood resilience assessment model developed by Bi et al. (2024) as background context. The overall research framework is presented in Fig. 3.

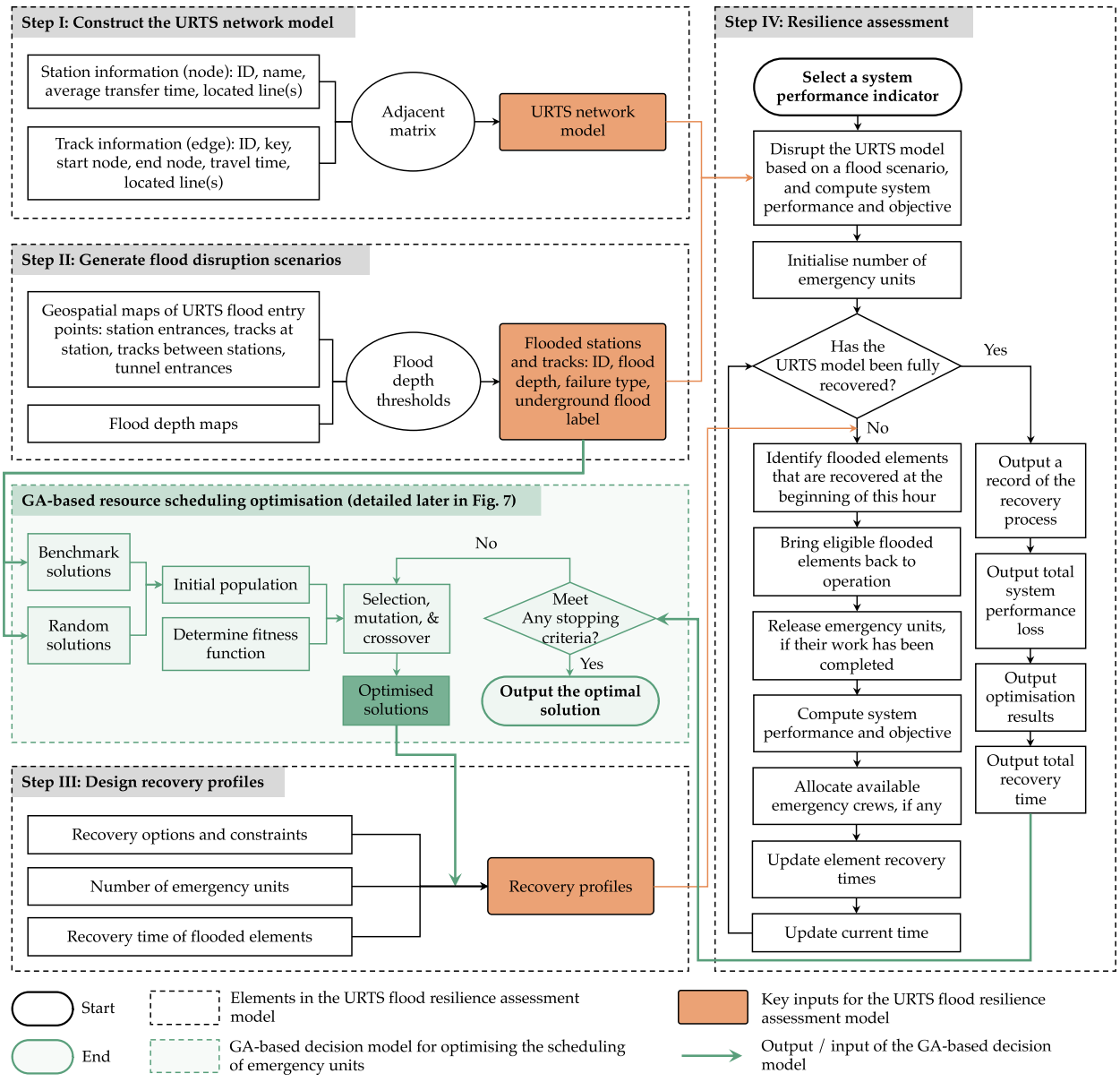

Fig. 3. Research framework. Step I: construct a network model to represent the URTS. Step II: generate flood disruption scenarios using flood depth maps. Step III: design recovery profiles for modelling the dynamic recovery process, where GA-based resource scheduling optimisation is incorporated. Step IV: assess URTS flood resilience based on system performance under flood disruptions and evaluates optimisation performance.

3.1. URTS flood resilience assessment model

While various approaches have been developed to measure the resilience of transport infrastructure, many studies rely on the resilience triangle curve to quantify system resilience based on performance loss caused by disruptions (as reviewed in Bi et al. (2023) and Hu et al. (2024)). Proposed by Bruneau et al. (2003), this conceptual model, as presented in Fig. 4, suggests that greater resilience within a system corresponds to lower total performance loss during a disruption. It communicates that resilience involves not only understanding the immediate impacts when a disruption occurs, but also the effectiveness of the recovery process. The total performance loss reflects the impacts on system operations and can be translated into economic or social impacts (Goldbeck et al., 2019).

Leveraging this conceptual model, Bi et al. (2024) recently developed a URTS flood resilience assessment model to evaluate performance loss and other impacts of flood disruptions. This model captures a considerable level of system complexities and dynamics, systematically considering the general engineering design features, network topology, operational performance, flood disruption scenarios, and recovery profiles. Unlike most current studies that rely solely on theoretical topological attributes to assess transport resilience (Henry et al., 2021; Ma et al., 2022; Martello et al., 2021; Yadav et al., 2020; Zhang & Ng, 2021), this model offers more practical and actionable insights by quantifying performance loss, revenue loss, and recovery time. The model constitutes four components: (1) select a system performance indicator, (2) construct a URTS network model, (3) generate flood disruption scenarios, and (4) design recovery profiles.

3.1.1. System performance indicator

The appropriate metric for assessing resilience should relate to the performance and services most critical to the transportation agency's mission, typically aligning with business continuity objectives (Transportation Research Board, 2021). As previous discussed, topological attributes are too abstract to satisfy this practical requirement. Given the fundamental objective of URTSs is to provide passenger travel

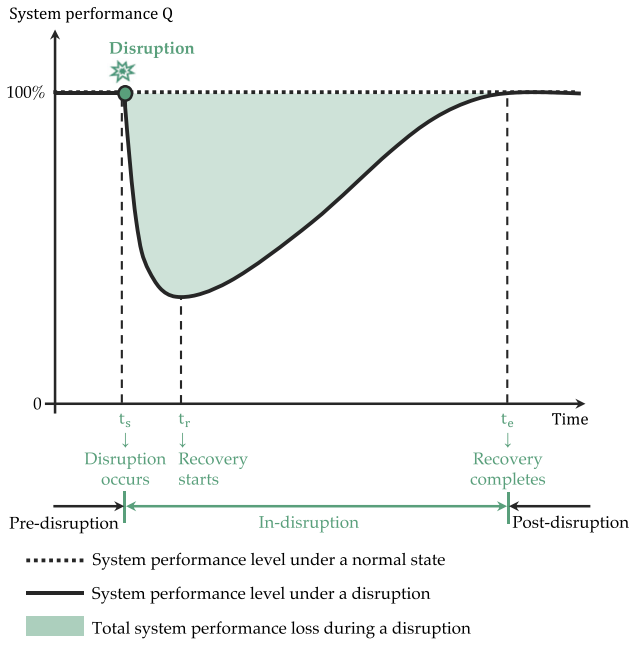

Fig. 4. Resilience triangle curve (Bruneau et al., 2003).

services, the selected URTS performance indicator in this study is the level of satisfied travel demand. This indicator not only directly reflects the system's core operational mission but also effectively captures multiple dimensions of infrastructure resilience. Specifically, the ability of URTSs to provide available and practical routes for passengers to travel indicates the physical connectivity of the URTS network (i.e., physical dimension). The level of satisfied travel demand signals operational performance (i.e., operational dimension). Unsatisfied travel demand resulting from service disruptions leads to direct revenue loss (i.e., direct economic dimension) and interruptions to passenger travel (i.e., touching on the social dimension). Moreover, a reduction in unsatisfied travel demand reflects the ability of asset operators to deploy resources and make effective recovery decisions (i.e., organisational dimension). By aggregating these dimensions, this indicator allows a practically meaningful quantitative assessment of URTS flood resilience.

When extreme floods disrupt the system, some of the planned travel cannot be satisfied due to unavailable routes or excessive service delays. In this case, resilience R can be quantified as the total loss of satisfied travel demand during the disruption duration $[t_s, t_e]$:

$$R = \int_{t_s}^{t_e} [Q(t) - Q'(t)]\, dt \tag{1}$$

where t_s refers to the time when disruption occurs and t_e refers to the time when recovery is completed. In this study, time t represents a specific hour of the day. $Q(t)$ and $Q'(t)$ denote the hourly satisfied travel demand in a normal state and under a disruption, respectively. The equation of $Q'(t)$ is presented below, where $N(t)$ refers to the total journey planned at time t, and $d_i'(t)$ indicates the satisfaction of journey i under disruptions.

$$Q'(t) = \sum_{i=1}^{N(t)} d_i'(t) \text{ , where } d_i'(t) = \begin{cases} 1, & \text{if journey } i \text{ at time } t \text{ is completed} \\ 0, & \text{if journey } i \text{ at time } t \text{ is disrupted} \end{cases} \tag{2}$$

The model assumes that passengers would take the shortest path for their planned travel, which refers to the route that requires the least amount of travel time, considering station dwell times, station transfer times, and travel times on the tracks. It incorporates the consideration of traffic redistribution through allowing rerouting and mode switching across rail transit services. When disruption occurs, the satisfaction of each journey requires two conditions: (1) there should be at least one path connecting the origin and destination stations of the journey, and (2) when the original shortest path is disrupted, the delay on the alternative shortest path should not exceed a practically acceptable duration. This delay threshold is set as a simplified measure to consider changes in passenger routing behaviours, as passengers may choose other transport or cancel their trips. The acceptable delay threshold in this study is set at $\Delta T = 30$ minutes. This follows Transport for London (TfL)'s practice of offering full refunds for journey delays exceeding 15 or 30 min during normal service operations, depending on the network section (Transport for London, 2023c, 2023h). Although delay refunds do not apply to weather-related disruptions, a 30 min delay serves as a reasonable benchmark for identifying service inadequacies that lead to unsatisfied demand, justifying its adoption in this analysis.

3.1.2. URTS network model

To model whether travel demand can be met based on these two conditions, a URTS network model, $G = (V, E, W)$, is constructed to model system performance during the entire disruption duration. $V = \{v_i \mid i = 1, 2, \dots n\}$ refers to a set of n nodes representing stations that feature multiple structural components, including entrances, concourse, stairways, platforms, and tracks within stations. $E = \{e_{ij} = (v_i, v_j) \mid i, j = 1, 2, \dots, n; i \neq j\}$ is a set of edges representing tracks that connect two adjacent stations. $W = \{w_{ij} \mid i, j = 1, 2, \dots, n; i \neq j\}$ is a set of edge weights that signal the travel time on each track. The network topology is featured with an adjacent matrix A composed of elements $A_{ij} (1 \leq i, j \leq n)$:

$$A_{ij} = \begin{cases} w_{ij}, & \text{if } v_i \text{ and } v_j \text{ are directly connected} \\ 0, & \text{if } v_i \text{ and } v_j \text{ are not directly connected} \end{cases} \tag{3}$$

where a non-zero $A_{ij} = w_{ij}$ denotes a direct connection between nodes v_i and v_j via an edge with a weight of w_{ij} and a zero $A_{ij} = 0$ indicates they are not directly connected. The network model is an undirected graph, meaning for each edge e_{ij} it is possible to travel from v_i to v_j as well as from v_j to v_i.

3.1.3. Flood disruption scenarios

Flood disruption scenarios are generated to model service disruption effects of flooding using the URTS network model. First, geospatial maps of URTS flood entry points are overlaid with flood depth maps to identify stations and tracks at risk and determine their flood depths. These flood entry points include (1) station entrances and (2) tracks within stations for identifying station flooding (corresponding to node failures), as well as (3) tracks between stations and (4) tunnel entrances for detecting track flooding (corresponding to edge failures). Each flooded element has a label indicating whether it pertains to underground flooding. This distinction affects the required recovery times and feasible recovery methods, which are further elaborated in Section 3.1.4. Following this, flood depth thresholds need to be established at levels beyond which the element becomes malfunctional due to flooding.

Flooding at different locations disrupts URTS operations in varying ways. For station flooding, flooding that only affects the station concourse can cause station closure as it is not safe for passengers to enter or exit, but trains can still pass through the station without making a stop. To model such disruption effects, the node representing this station is removed from the URTS network model, while edges connected to this node are removed automatically. Meanwhile, a temporary node along with adjacent edges is added at this location in the network model to enable trains to pass through. Conversely, flooding that damages tracks within stations can obstruct the passage of trains. In this case, this node is removed from the network model to represent such disruptions. This is similar to flooding affecting tracks between stations, where trains cannot pass. When modelling this effect, the edge representing this flooded track between stations is removed

Table 2
Recovery methods.
Source: Adapted from (Bi et al., 2024).

Recovery method	Applicability	Resource availability	Efficiency & priority
Pumped out by an emergency crew	Any situation.	Limited number of emergency crews.	⋆ ⋆ ⋆
Manually cleaned by staff at stations	Any situation except: – Where the water depth is overly deep (0.6 m is adopted in this study). – Underground flooding.	Stations are usually equipped with staff who can perform this task.	⋆⋆
Naturally recede	Any situation except: – Underground flooding.	No resource required.	⋆

from the network model. Additionally, track failures occurring between stations can lead to cascading impacts on the availability of turning points or substations for adjacent tracks, which could cause partial line suspension in practice. According to Bi et al. (2024), this is modelled by suspending two adjacent tracks (i.e., edges) on each side of the flooded track, based on recommendations from Transport for London (TfL) professionals.

3.1.4. Recovery profiles

Recovery profiles serve as guidance for modelling the dynamic recovery process of URTSs from flood disruptions. They take into account (1) methods used to clean up floodwater, (2) recovery times required for elements with varying extents of flood depth, and (3) resource scheduling priorities.

Regarding recovery methods, as illustrated in Table 2, the most efficient way to clear floodwater is to have it pumped out by an emergency crew. This applies to any situation; however, the number of emergency crews is often limited. When emergency crews are not readily accessible, an alternative method is for station staff to manually clear water using mops and buckets. In this study, it is assumed that stations are equipped with abundant staff who can perform this task. However, due to health and safety reasons, this does not apply to flooding in underground stations or tunnels, or in cases where the floodwater is overly deep for safe access. In other cases, water can be left to recede naturally, such as floodwater at at-grade tracks located in an open environment. However, this does not apply to underground flooding either. When applicable and available, the priority of these three recovery methods is directly proportional to their efficiency. It should be noted that only one recovery method can be applied to each flooded element at a time, which is a reasonable simplification that aligns with the general practices informed by practitioners.

As efficiency varies among the three recovery options, employing different methods impacts the recovery time. For the same level of flooding, the required recovery times are ordered as $t_p < t_m < t_n$, where t_p, t_m, and t_n represent the times for pump, manual, and natural recovery, respectively. Additionally, an element's recovery time could be dynamic, depending on when and what recovery method is applied. For example, for a station with a low flood level and a medium resource scheduling priority, station staff can be immediately available to conduct manual recovery before an emergency crew becomes available and arrives to accelerate the process using pumps. In this case, the total time T spent on recovering this station is computed based on:

$$T = t_0 + \left(1 - \frac{t_0}{t_m}\right) t_p \tag{4}$$

where t_0 is the time spent on manual recovery before receiving an emergency crew, t_m is the total time required for manual recovery alone, and t_p is the total time required for recovery solely by pumping. Apart from recovery methods, these recovery times t_p, t_m, and t_n also vary by the extent of flood depth, which can reasonably indicate the extent of flood damage (Martello et al., 2023). t_p, t_m, and t_n for each level of flood depth and each type of recovery method are estimated for the case study based on available historical flood incident records (detailed later in Section 4.2). t_0 is recorded as the recovery simulation progresses.

3.2. GA-based recovery resource scheduling optimisation

As introduced above, the natural recession of floodwater requires no specific resources. While manual recovery requires station staff as a resource, it applies only when the floodwater depth is less than 0.6 m due to health and safety concerns, and practical experience suggests that it is a reasonable simplification to assume stations are usually staffed to perform this task, meaning that resource constraints are not a significant consideration. Given that the availability of the most efficient and applicable resource – emergency crews – is often limited, optimising the scheduling of these emergency crews is crucial for enhancing recovery efforts and minimising post-flood impacts. Therefore, this study utilises GAs to assess its effectiveness. Through iterations known as generations, GAs evolve a population of potential solutions towards an increasingly optimal solution. This section introduces how the algorithm is applied to optimise the scheduling of limited emergency crews.

3.2.1. Problem description

The objective of optimising recovery resource scheduling is to minimise post-flood impacts of URTS service disruptions. By leveraging the URTS flood resilience assessment model described in Section 3.1, all unsatisfied travel demand during the disruption period can be identified. This provides a starting point for understanding post-flood impacts from an operational performance perspective. To better align with the practical needs of transit agencies in promoting resilience planning investments, revenue loss can be estimated by integrating corresponding calibrated peak and off-peak fare rates with each instance of unsatisfied travel demand. This approach offers valuable insights into the direct economic impacts of flood-induced service disruptions, translating the optimisation objective into minimising total revenue loss, L, over the disruption period. The mathematical formulation of this optimisation problem is presented below:

$$\min L = \sum_{t=t_s}^{t_e} \Bigg[\underbrace{\sum_{i=1}^{N(t)} f_i(t)}_{F(t)} - \underbrace{\sum_{i=1}^{N(t)} d_i'(t) \cdot f_i(t)}_{F'(t)} \Bigg] \tag{5a}$$

subject to:

$$\sum_{\ell \in \mathcal{L}} x_{\ell,t} \;\leq\; k, \quad \forall\, t \in \mathcal{T} \tag{5b}$$

$$z_{\ell,t} = 1 \iff \sum_{\tau=t_s}^{t} x_{\ell,\tau} \;\geq\; M_\ell, \quad \forall\, \ell \in \mathcal{L},\ \forall\, t \in \mathcal{T} \tag{5c}$$

$$d_i'(t) = 1 \iff \exists\, p_{o_i \to d_i'} : \left(z_{\ell,t} = 1\ \forall \ell \in p\right) \wedge \left(T_i'(p_{o_i \to d_i'}) \leq T_i + \Delta T\right) \tag{5d}$$

where $F(t)$ and $F'(t)$ represent the hourly revenue in a normal state and under disruptions, respectively. t_s is the time when disruption occurs, and t_e is the time when recovery is completed. $f_i(t)$ refers to

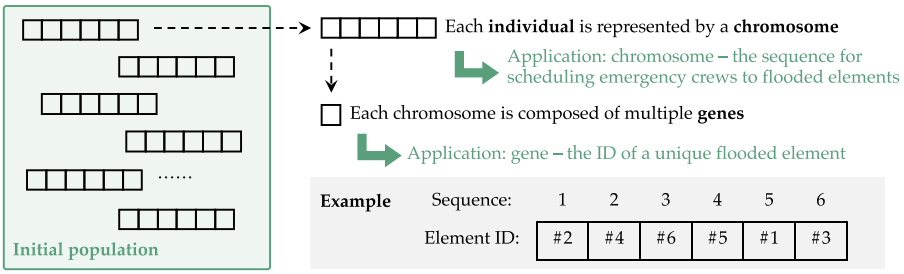

Fig. 5. Explanation of chromosomes and genes in this context.

the calibrated fare rate of journey i at time t. Note that calibrated fare rates differ between peak (7–9 a.m. and 5–7 p.m.) and off-peak periods. $d_i'(t)$ indicates the satisfaction of journey i, as introduced in Eq. (2).

Crew availability is enforced through Eq. (5b), ensuring that at any time t, the number of elements ℓ assigned an emergency crew does not exceed the total number of available crews k. The binary decision variable $x_{\ell,t} \in \{0,1\}$ specifies whether element ℓ is actively under repair by a crew at time t. By choosing which elements to assign a crew and when, the solver directly controls the restoration timeline, determining when each element becomes fully operational ($z_{\ell,t} = 1$). The *element restoration logic* is captured in Eq. (5c), which sets $z_{\ell,t} = 1$ once element ℓ has accumulated the required M_ℓ units of repair time, indicating that it is fully operational. The *journey feasibility condition* in Eq. (5d) states that a journey i is considered satisfied at time t (i.e., $d_i'(t) = 1$) if and only if there exists at least one path p from origin o_i to destination d_i such that (1) all elements ℓ along path p are operational ($z_{\ell,t} = 1$), and (2) the total travel time satisfies $T_i' \leq T_i + \Delta T$, where ΔT is the allowable delay threshold (as introduced in Section 3.1.1, $\Delta T = 30$ minutes), T_i represents the travel time of journey i in the normal state, and T_i' is the travel time during disruptions.

3.2.2. Fitness function

According to natural selection's principle of "survival of the fittest" (Mitchell, 1998), individuals best adapted to their environment are most likely to survive and reproduce. In GAs, when evolving to the optimal solution during iterations of generations, this principle translates to a higher fitness value f signifying a superior solution. To align with optimisation objective presented in Eq. (5a), the fitness value f is computed as the inverse of the total revenue loss, as presented in Eq. (6). The objective of maximising f implies that a lower total revenue loss corresponds to a better solution.

$$f = \frac{1}{\sum_{t=t_s}^{t_e'} \left[F_i(t) - F_i'(t) \right]} \tag{6}$$

3.2.3. Genes and chromosomes

Each individual in a population is represented by a chromosome, as shown in Fig. 5. Each chromosome is composed of multiple genes arranged in a specific sequence that collectively represents a solution to the optimisation problem. In this study, each gene represents a decision variable, which corresponds to a unique flooded element identified by its ID. Accordingly, each chromosome symbolises the prioritisation order of these flooded elements for receiving an emergency crew. The size of gene space is equal to the number of flooded elements in each scenario. The example given in Fig. 5 illustrates that, for instance, when only two emergency crews are available, element #2 and #4 are prioritised to receive them. Meanwhile, other elements may proceed with manual or natural recovery methods, if feasible. If not, they must wait in the queue for an available crew.

3.2.4. Benchmark solutions

Benchmark solutions are generated to form part of the initial population and to evaluate the optimisation performance. This study employs four benchmark solutions, each based on an importance indicator of flooded elements, to establish their priorities for receiving an emergency crew. Elements of higher importance are prioritised for earlier assignment of an emergency crew. Indicators for measuring node importance are described in Table 3, including three variations of betweenness centrality and daily passenger flow at stations. The importance of edges is determined by the maximum importance of its two connecting nodes. As benchmark #3 is employed as the resource scheduling solution in the original model in Bi et al. (2024), it is adopted as the baseline to evaluate the optimisation performance of GA-derived solutions in the case study.

3.2.5. Optimisation process

As presented in Fig. 6, the optimisation process begins with generating the initial population with S solutions. which consists of a random solutions and b benchmark solutions. The random solutions represent random sequencing of the IDs of all flooded elements. The benchmark solutions adopt the four sequences determined based on Table 3. Hence, $b = 4$ in this study. These benchmark solutions are utilised to initiate the exploration from a good starting point, thereby reducing the computation time. The fitness value is then computed to evaluate the quality of each solution.

Subsequently, p solutions are selected as parents through the roulette wheel selection method, where the probability of each solution being selected as a parent is proportional to its fitness value (Linder, 2022). Following this, a single-point crossover is conducted to produce offspring. Duplicate genes need to be addressed as each flooded element is unique (see Fig. 7(a)). Then, each offspring experiences a "swap" mutation, whereby a selected percentage of genes are randomly chosen, and their values are exchanged (see Fig. 7(b)). After mutations, p new solutions are obtained as part of the next generation and their fitness values are computed. It is worth noting that in this study, p is expected to be smaller than S (i.e., not all initial solutions are selected as parents), which is an additional setting for reducing computation time and also reflects the principle of natural selection.

To keep a fixed size of the population and avoid losing the best solutions during evolution, this study applies the elitist strategy, meaning $(S-p)$ best solutions in each generation are passed on to form part of the next generation. The evolution of generations keeps proceeding until reaching any stopping criteria and a near-optimal solution is hence obtained. The stopping criteria is designed to maximise the exploration of the optimal solution while considering constraints on acceptable computation time during this experimental stage, though it may not necessarily be feasible for real-time decision-making.

Table 3
Benchmark solutions.

ID	Importance indicator	Explanation	Emphasis	Baseline
#B1	Unweighted node betweenness centrality	It measures the importance of a node based on how often it is located on the shortest paths between any node pairs in an unweighted network. The betweenness centrality of node v, $g(v)$, is formed in: $$g(v) = \sum_{\substack{s,t,v\in V \\ s\neq t\neq v}} \frac{\sigma(s,t\|v)}{\sigma(s,t)} \quad (7)$$ where $\sigma(s,t\|v)$ is the number of times that node v lies on the shortest path between nodes s and t and $\sigma(s,t)$ is the total number of shortest paths between nodes s and t. In unweighted networks, the shortest path between a node pair is the one with the least number of edges.	Topological attribute	
#B2	Time-weighted node betweenness centrality	Similar to the one above except edges in the network are weighted by travel times. In time-weighted networks, the shortest path between a node pair is the one with the least amount of travel time, which aligns better with reality.	Improved topological attribute	
#B3	Demand-weighted node betweenness centrality	Similarly, edges are weighted by travel times and the shortest path is the one with the least amount of travel time. In addition, to integrate operational importance into this topological importance, the level of travel demand between each node pair, $d(s,t)$, is incorporated into the betweenness centrality equation to indicate how busy the shortest path of the node pair is, as shown in : $$g'(v) = \frac{1}{D}\left(\sum_{\substack{s,t\in V \\ s\neq t\neq v}} \frac{\sigma(s,t\|v)d(s,t)}{\sigma(s,t)}\right) \quad (8)$$ where D refers to the travel demand between all node pairs.	Combination of topological attribute and operational performance	✓
#B4	Daily passenger flow at stations	It measures the average number of passengers entering and exiting a station during a day, which signals the operational performance.	Operational performance	

4. Case and data descriptions

4.1. The London URTS

The London URTS is a highly complex network that is vulnerable to surface water flooding (Greater London Authority, 2018). As presented in Fig. 8(a), the London URTS network model constitutes 443 nodes representing stations and 533 edges representing tracks between stations, covering 15 lines of the London Underground (LU), the London Overground (LO), the Dockland Light Railway (DLR), the Elizabeth Line (EL), and the London Trams (LT).

The target system performance level under a normal state employs a total of 5,342,647 journeys between 51,905 origin–destination (OD) station pairs on a typical autumn weekday in London in 2019 (see Fig. 8(b)). This dataset, readily accessible from Transport for London (2020), involves the number of journeys in every 15 min period throughout the day and assumes a perfect train schedule being operated. These data at 15 min intervals are aggregated into hourly segments for analysis (see Fig. 8(c)). Details of the OD travel demand data and other data (e.g., network topology, travel time between stations, and fare rates for revenue estimation) used in this case study are provided in Table A.1 in Appendix A.

4.2. London flood scenarios

This study adopts the 30-year, 100-year, and 1,000-year flood disruption scenarios identified by Bi et al. (2024), utilising the surface water flood risk maps produced by the UK Environment Agency (Department of Environment Food & Rural Affairs, 2021). The 30-year flood risk scenario represents a relatively high probability circumstance that could serve as a foundational baseline for designing flood risk mitigation strategies for protecting the infrastructure. The 100-year flood risk scenario, with a slightly lower probability but higher potential impact, is crucial for identifying critical assets that are vulnerable at this level and thus demand more rigorous safety measures. The 1,000-year flood risk scenario, characterised by its low probability yet catastrophic potential, is not beyond the realm of possibility (as observed in Australia in 2022) and serves as an extreme stress test for enhancing emergency response and recovery strategies. These three progressively severe flood scenarios offer a diverse range of conditions to stress-test the system and understand potential effectiveness of optimising emergency crew scheduling in mitigating post-flood impacts.

These flood maps classify flood depths as 0, 0–0.15 m, 0.15–0.3 m, 0.3–0.6 m, 0.6–0.9 m, 0.9–1.2 m, and >1.2 m. Having a reasonably high horizontal grid resolution of 2 m, these maps allow the identification of location-specific flood exposure of URTS flood entry points. For the studied London URTS, these flood entry points include 735 station entrances, 398 tunnel entrances, 721 track sections within stations, and 933 track sections between stations.

Derived from discussions with TfL professionals, a threshold of 0.3 m is used for flood-induced failure at non-underground station entrances, tracks within stations, tracks between stations, and tunnel entrances. For underground station entrances, a threshold of 0.6 m is applied, meaning that when flood depth at the station entrance exceeds 0.6 m, water can flow down the staircases into the underground space and disrupt operations. Numerous nodes and edges are identified as flooded in each scenario, as shown in Fig. 9 and Table 4. The time required for each element to recover varies from 3 h to 48 h, depending on the flood depth and the recovery method employed. These recovery times are estimated by consulting experienced professionals at TfL with referencing its historical flood incident records. Detailed assumptions on recovery times are provided in Table B.1.

It should be noted that these maps are generated through modelling "current day" scenarios and thus do not account directly for climate change impacts. It is anticipated that London will experience more intense rainfall and risk of flash flooding based on the current expected climate change trajectory (Boyd et al., 2024). The stated frequency periods of the scenarios used here are likely to underestimate the system-level risk, which increases the value of conducting the recovery modelling laid out in this study.

Table 4
Number of flooded elements of the London URTS in each flood scenario.
Source: Adapted from Bi et al., 2024

Element type	Flood depth	Number of flooded elements in each scenario		
		30-year flood	100-year flood	1,000-year flood
Nodes	0.3-0.6 m	28	39	51
	0.6-0.9 m	9	27	27
	0.9-1.2 m	3	6	19
	>1.2 m	4	10	49
	Total	44	82	146
Edges	0.3-0.6 m	50	61	48
	0.6-0.9 m	15	43	41
	0.9-1.2 m	5	12	43
	>1.2 m	11	30	96
	Total	81	146	228

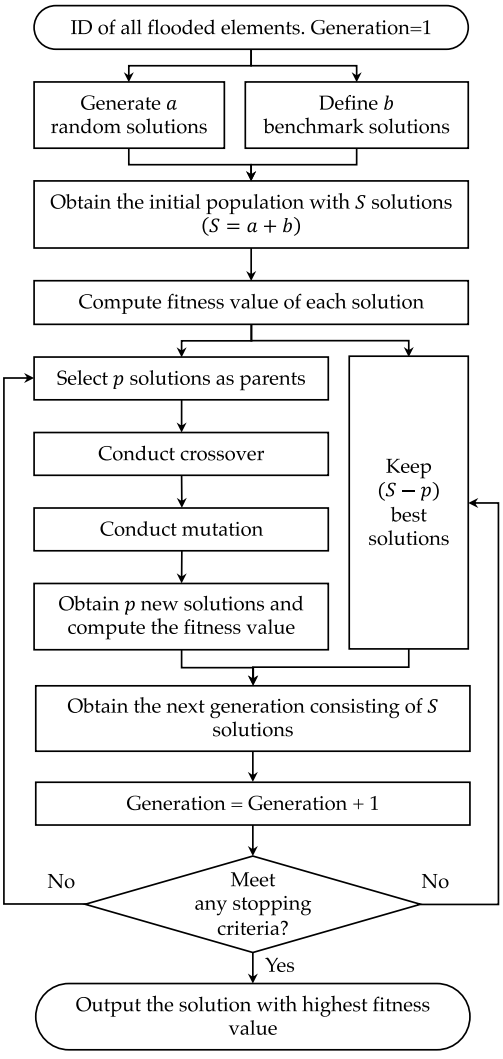

Fig. 6. Genetic algorithm-based resource scheduling optimisation.

4.3. Simulation settings

The simulation follows four main procedures to assess total unsatisfied travel demand and revenue loss resulting from flood-induced service disruptions. First, it constructs a URTS network model. Second, at the beginning of a selected hour, this URTS network model is disrupted by disabling all flooded nodes and edges in the ways as described in Section 3.1.3. The level of satisfied travel demand and ticket revenue for this hour are computed. Third, for each solution in the population of the GA-based model, an individual recovery is simulated to compute the fitness value of this solution. Recovery commences at the beginning of the next hour, and the simulation executes the following steps at each hour until all elements are restored and operational (also refer to Step IV in Fig. 3): (1) check flooded elements that have been recovered at the beginning of this hour (i.e., time spent on recovery is equal to total time required for recovery), (2) bring eligible flooded elements back to operation, (3) release emergency crews that have completed their work and set one hour time slot (Transport for London, 2024b) for travel to the next location—an assumption made to manage model complexity, (4) compute satisfied travel demand and ticket revenue for this hour, and (5) allocate available emergency crews to flooded elements that have not yet fully recovered, based on the scheduling solution given by the GA-based decision model. After the completion of recovery, the total unsatisfied travel demand and revenue loss during the disruption duration are calculated by comparing with the values in a normal state. This network modelling process is constructed using the Python library NetworkX.

Following this, the fitness value of each solution in the population of the GA-based model is computed as the inverse of the corresponding revenue loss. Unless a stopping criteria is reached, all solutions then experience selection, mutation, and crossover to generate a new population of solutions for fitness computation. The evolution of generations keeps proceeding until reaching a stopping point signalled by either the number of generations reaching 1,000 or the best solution remaining unchanged for 50 consecutive generations. This GA-based optimisation is constructed using the Python library PyGAD.

The parameter settings are summarised in Table 5. Based on consultation with professionals in TfL's Pump Department and Emergency Response Unit, this study assumes that 15 emergency crews are available to work simultaneously when the system is disrupted by large-scale floods. The resource scheduling optimisation is conducted for these 15 emergency crews. To ensure that the simulation time remains within acceptable limits while preserving solution diversity, the population size is set at ten. In addition to the four benchmark solutions introduced in Table 3, six random solutions are included to ensure diversity in the first generation. To maintain computational feasibility while ensuring adequate genetic variation, six solutions are selected as parents for crossover. Four elitists are passed on to the next generation to keep the population size at ten. Ten percent of the genes are allowed for mutation. This relatively high mutation rate helps avoid premature convergence to local optima. Simultaneously, the implementation of an elitist strategy ensures that high-quality solutions are retained throughout the process. The size of the gene space is 125, 228, and 374 in three scenarios, respectively, equal to the number of flooded elements. While there are no universal settings of these parameters, the current configuration demonstrates consistent optimisation performance

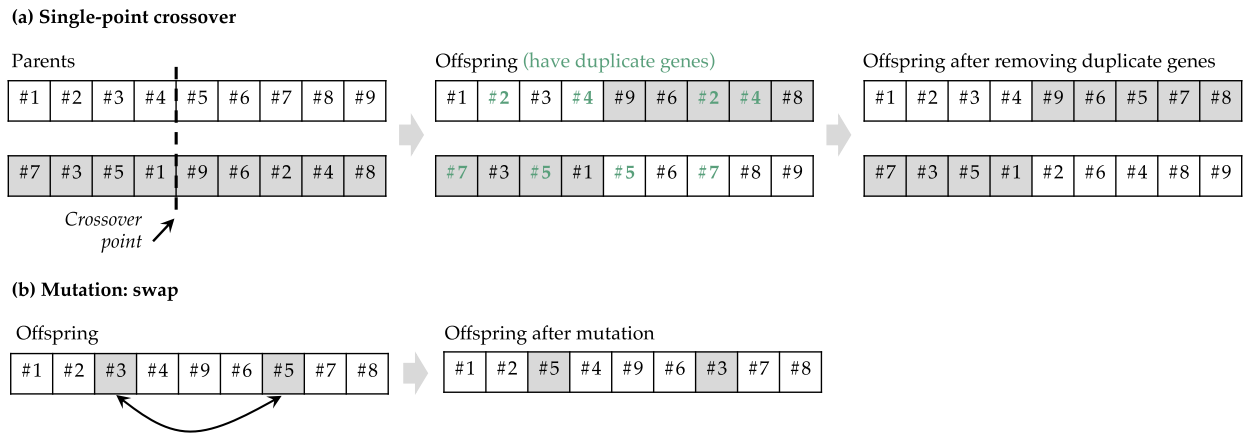

Fig. 7. Settings of crossover and mutation.

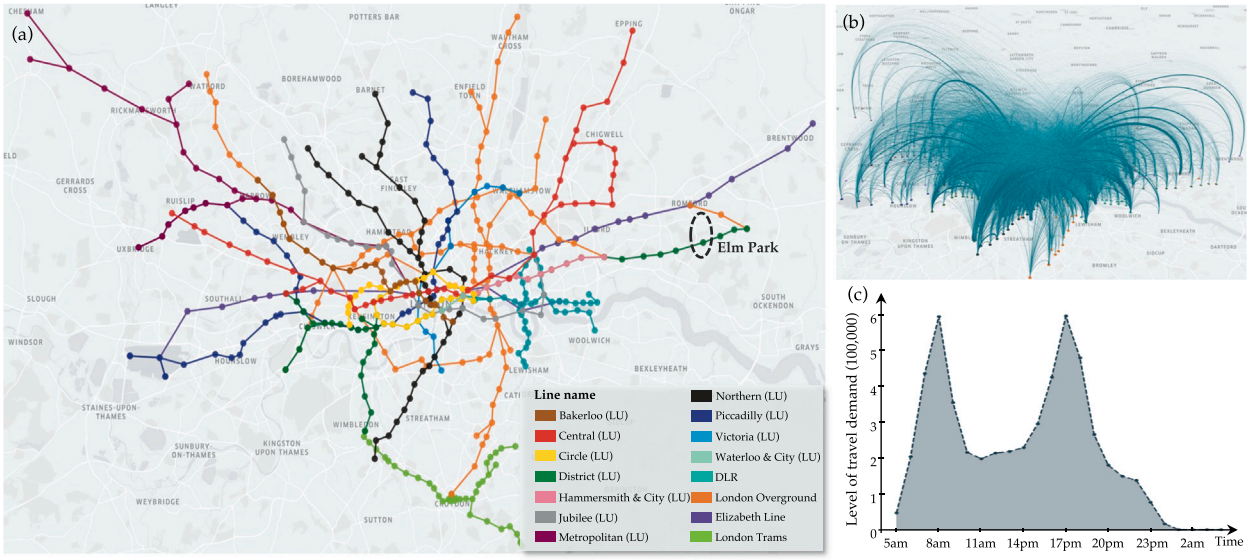

Fig. 8. The London URTS: (a) lines; (b) OD pairs of daily travel demand; (c) level of hourly travel demand.

across all tested scenarios, effectively balancing solution quality with computational feasibility.

4.4. Benchmark results

According to the guidance provided in Table 3, four sets of importance indicators for the elements in the London URTS are computed based on the topology of the London rail transit network, real travel times between adjacent stations, and real OD travel demand between stations (for data details, see Table A.1). The total revenue loss and unsatisfied travel demand of the four benchmark solutions are presented in Table 6. Benchmarks #B1 and #B2, which are created based on pure topological attributes, generally perform worse in all scenarios than the other two benchmarks that take account of operational performance (either travel demand between stations in benchmark #B3 or passenger flow at stations in benchmark #B4). Benchmark #B4, which relies solely on an operational performance indicator, offers the best results in the 30-year flood scenario, but its effectiveness declines as the extent of flood damage increases, as depicted in Fig. 10. On the contrary, benchmark #B3, which integrates betweenness centrality with operational performance, demonstrates progressively enhanced effectiveness as the severity of flood increases and provides the best results in the 1,000-year flood scenario. This suggests that while considering operational performance is critical for reducing total revenue loss, the topological attribute begins to show promise in larger-scale disruptions of the network, as it is more effective in capturing the dynamic and complex impact of network connectivity changes on system performance.

5. Results

5.1. Diversity of solutions

During the preliminary testing phrase, approximately 20 tests were carried out, all of which consistently demonstrated a clear and stable trend towards optimisation. Given the significant computational time required for each full simulation, it was determined that conducting six complete simulations for each scenario would provide a reasonable basis for ensuring the reliability and robustness of the results.

The optimisation performance is depicted in Fig. 11, which shows an incremental increase in the fitness value of the best solution among each generation and a corresponding decrease in the total revenue loss. In each scenario, the simulations stop at different generations, and some simulations stop early but end up with higher fitness values (e.g., simulation #GA3 in the 30-year flood scenario) compared to other simulations that stop late, indicating the inherent randomness of GAs when seeking the near-optimal solutions.

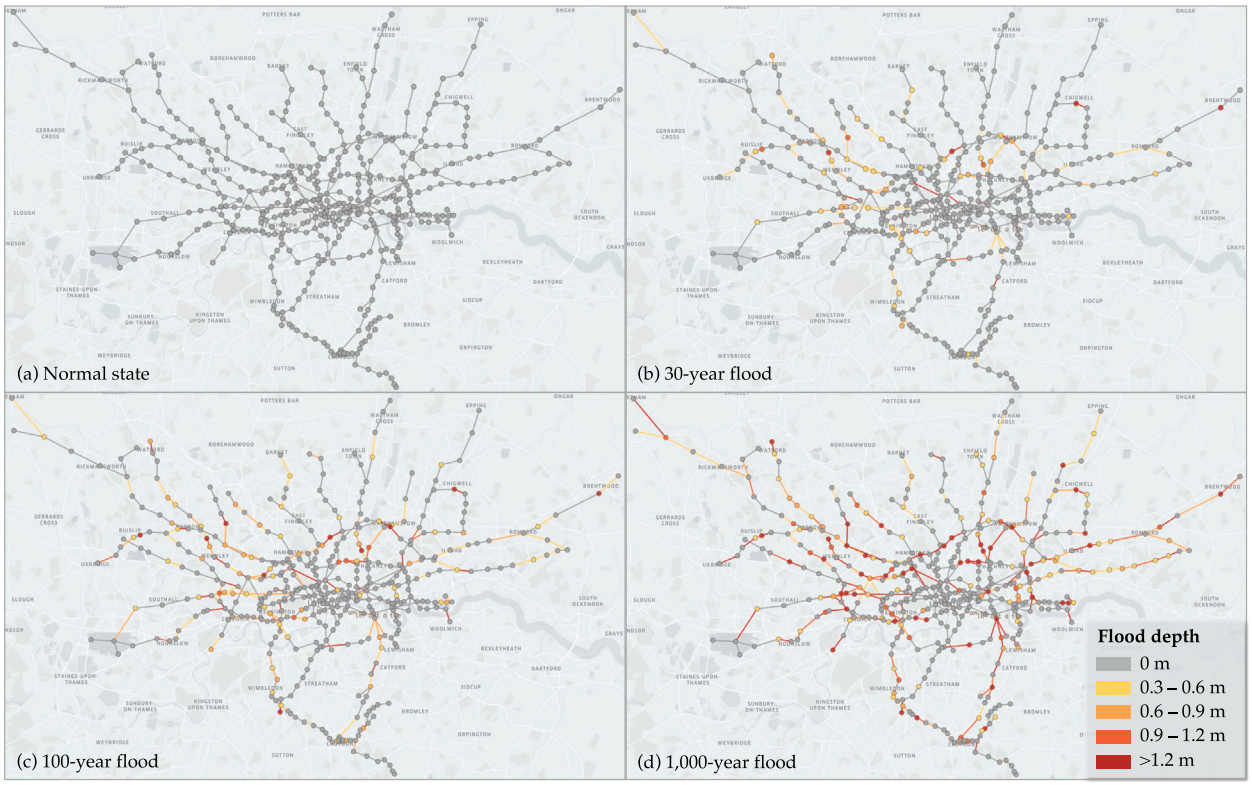

Fig. 9. Flooded stations and tracks of the London URTS with their flood depths (Bi et al., 2024).

Table 5
Parameter settings.

Component	Parameter	Value
Network modelling for resilience assessment	Target system performance level	5,342,647 daily journeys
	Acceptable journey delay	$\Delta T = 30$ minutes
	Number of adjacent edges of the flooded edge to suspend	2 on each side of the flooded edge
	Start time of disruption	5 p.m. on a weekday
	Start time of recovery works	6 p.m. (one hour later)
	Travel time of an emergency crew to next location	1h
	Number of concurrent emergency crews	$k = 15$
	Assumptions on element recovery times	Detailed in Appendix B
GA-based resource scheduling	Number of random solutions in the initial population	$a = 6$
	Number of benchmark solutions in the initial population	$b = 4$
	Population size	$S = 10$
	Number of parents selected for crossover	$p = 6$
	Number of elitists passed on to the next generation	$S - p = 4$
	Type of parent selection	Roulette wheel selection
	Type of crossover	Single-point crossover
	Type of mutation	Swap
	Percentage of genes for mutation	10%
	Gene space	Equal to the number of flooded elements
	Allow duplicate genes	False
	Stopping criteria	"Generation=1,000" OR "if the optimal solution remains unchanged for 50 consecutive generations"

The average Spearman's rank correlation coefficient (Spearman, 1961), also referred to as Spearman's ρ, is computed to measure the similarity between the six solutions in each scenario. The Spearman's ρ is 0.275, 0.106, and 0.250 in the three flood scenarios, respectively, suggesting a low positive correlation between the scheduling of elements across these solutions. This reflects the algorithm successfully explores diverse solutions within the wide search space, demonstrating its value in navigating a complex optimisation problem in the context of infrastructure system recovery following large-scale disruptions.

5.2. Optimisation results

The designed GA-based optimisation model exhibits satisfactory optimisation effectiveness in identifying near-optimal resource scheduling

Table 6
Results of benchmark solutions.

Benchmark solution	Total revenue loss (£1,000)			Total unmet travel demand (1,000)			Recovery time (h)		
	30-year flood	100-year flood	1,000-year flood	30-year flood	100-year flood	1,000-year flood	30-year flood	100-year flood	1,000-year flood
#B1	3,210	7,175	12,209	1,914	4,446	7,699	44	79	107
#B2	3,138	7,117	11,975	1,861	4,396	7,541	44	79	104
#B3	3,100	6,752	11,403	1,834	4,127	7,157	43	79	96
#B4	2,899	6,741	11,814	1,719	4,159	7,441	38	66	99

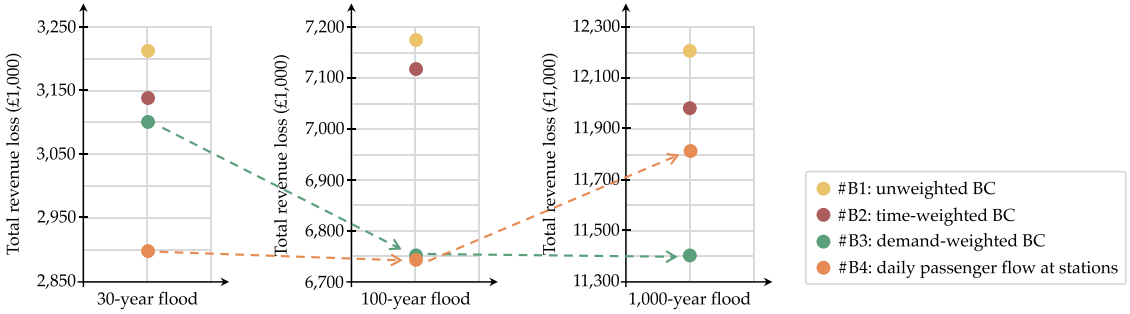

Fig. 10. Total revenue loss of benchmark solutions.

Table 7
Optimisation results of GA solutions (compared with baseline #B3)

GA optimised solution	Reduced revenue loss (£1,000)			Reduced unsatisfied travel demand (1,000)			Change in recovery time (h)		
	30-year flood	100-year flood	1,000-year flood	30-year flood	100-year flood	1,000-year flood	30-year flood	100-year flood	1,000-year flood
#GA1	336 (10.8%)	729 (10.8%)	677 (5.9%)	195 (10.7%)	416 (10.1%)	411 (5.7%)	+2	−3	+6
#GA2	332 (10.7%)	708 (10.5%)	712 (6.2%)	192 (10.5%)	407 (9.9%)	442 (6.2%)	+1	−10	−1
#GA3	384 (12.4%)	796 (11.8%)	810 (7.1%)	229 (12.5%)	463 (11.2%)	494 (6.9%)	+8	−8	+6
#GA4	351 (11.3%)	734 (10.9%)	779 (6.8%)	203 (11.0%)	427 (10.4%)	496 (6.9%)	−4	−10	+7
#GA5	302 (9.7%)	740 (11.0%)	812 (7.1%)	178 (9.7%)	432 (10.5%)	513 (7.2%)	0	−6	+6
#GA6	318 (10.3%)	541 (8.0%)	769 (6.7%)	186 (10.2%)	281 (6.8%)	464 (6.5%)	+8	−10	+6
Average	337 (10.9%)	708 (10.5%)	760 (6.7%)	197 (10.7%)	404 (9.8%)	470 (6.6%)	+2.5	−7.8	+5

solutions to reduce total revenue loss during disruptions. As illustrated in Table 7, compared with the optimisation baseline #B3, the total revenue loss can be reduced by an average of 10.9%, 10.7%, and 6.7% when exposed to the 30-year, 100-year, and 1,000-year flood risks, respectively. This effectively means that employing better emergency crew scheduling can save around £337K, £708K, and £760K in direct revenue loss in respective scenarios. These savings are substantial from the transit operator' perspective, demonstrating the significant potential for mitigating post-flood impacts to enhance URTS flood resilience.

The improvement in operational resilience not only translates into financial savings but also enhances the passenger experience by minimising disruptions to their planned journeys. With better scheduling solutions, the average unsatisfied travel demand can be reduced by around 197K, 404K, and 470K in each scenario. Fig. 12 provides an example of how the level of satisfied travel demand changes during the recovery process when different scheduling solutions are employed. It compares benchmark #B3 with the solution #GA3 in the 30-year flood scenario. Somewhat unintuitively, the solution #GA3 takes more time to complete the recovery process (so do some other GA solutions as shown in Table 7). Nevertheless, when aggregating the hourly satisfied demand into daily segments (see Fig. 12(b)), the "resilience triangles" more clearly reveal the benefit of applying the GA solution in reducing unsatisfied travel demand. This indicates that when the system performance is the key concern, a longer recovery time does not necessarily mean a worse recovery efficiency. It is worth prioritising resources to restore more critical elements in the system to get more service back as early as possible.

5.3. Identification of critical elements

Elements that consistently locate early in the scheduling sequence across different solutions should be considered critical (though this holds true in this specific disruption scenario, it does not necessarily applies to other disruptions where system dynamics could vary during recovery), as this suggests their relative priority in the recovery process is robust to the random exploration process of GAs. Fig. 13 plots the range of element sequence positions across the six GA solutions in the 30-year flood scenario, where the number of elements is manageable

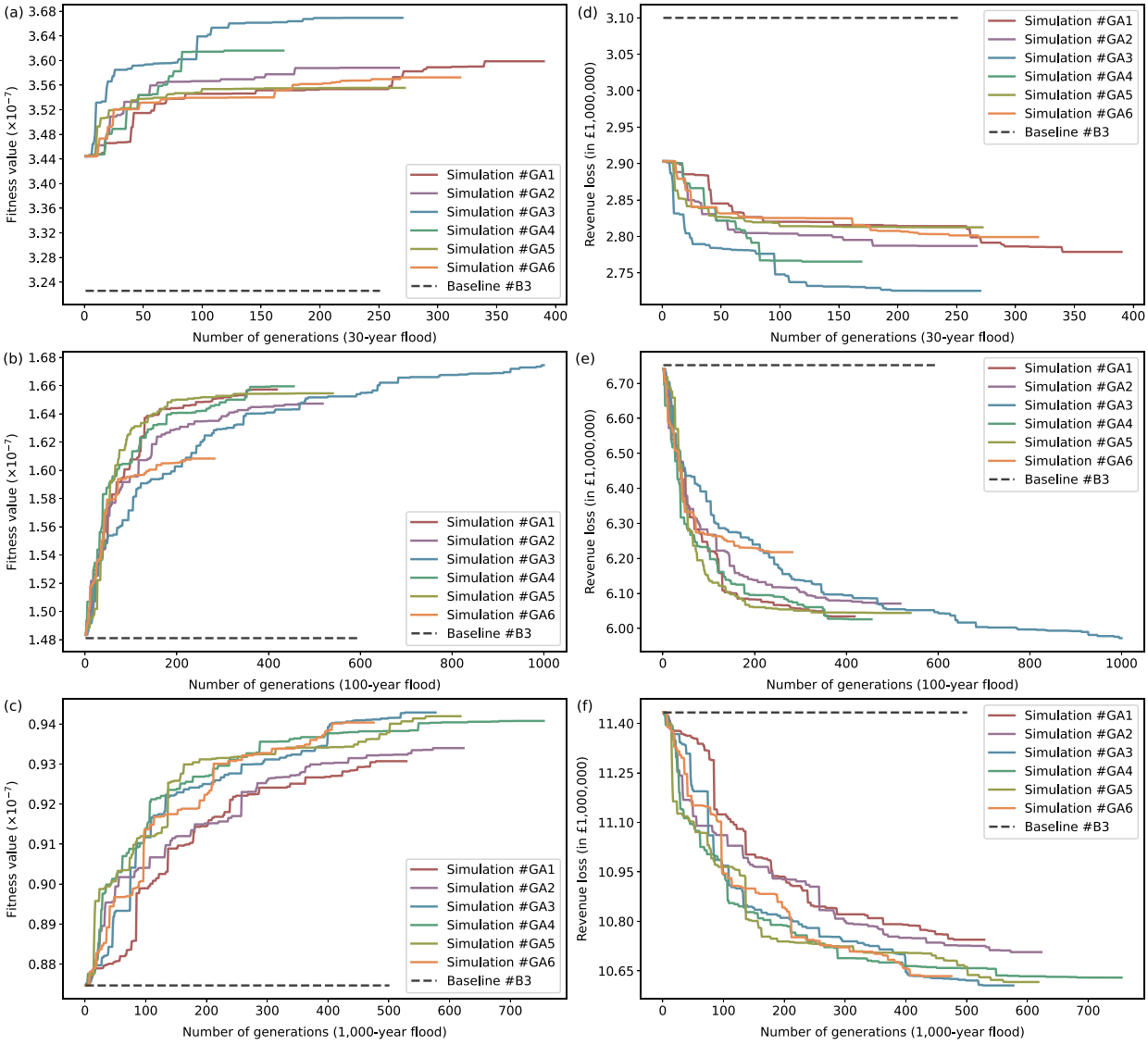

Fig. 11. Optimisation performance. (a)–(c) show the fitness value of the best solution in each generation for each scenario. (d)–(f) show the corresponding revenue loss of the best solution in each generation for each scenario.

for visualisation. Elements on the x-axis are arranged based on the span of their positions across six solutions, namely elements appearing earlier exhibit greater consistency in their sequence positions across different solutions. Although the positional consistency of most elements is low, a few elements in the bottom left corner of Fig. 13 show great consistency in their priority. Characteristics of elements that consistently rank in the top 20 are presented in Fig. 14, where element labels are anonymised for security considerations.

As highlighted in Fig. 14, most of the elements with consistent high priority are edges, with Edge #58 and Edge #53 constantly being the first two elements allocated with an emergency crew. Both edges carry a significant number of daily link load, which refers to the number of passengers travelling along this edge. Additionally, Edge #58 serves multiple lines, including the Circle Line, the Hammersmith & City Line, and the Metropolitan Line, as does Node #14, which is the interchange station of the Circle Line, the District Line, and the Piccadilly Line and is frequently located fifth in the scheduling solutions. Other critical elements warranting early attention include Edge #63, Edge #52, Edge #65, Edge #85, Edge #66, Edge #119, Node #3, and Edge #110. It is unexpected that Node #3 has a high priority, given its relatively low passenger flow and absence of interchange capabilities (see Fig. 8(a)). However, bringing this station back to operation helps restore the connectivity between the Hammersmith & City Line and the Elizabeth Line, which may reflect the complex system dynamics.

6. Discussion

6.1. Enriching the paradigm of disaster risk management

The notable reductions in revenue loss and disrupted passenger travel demonstrate the value of planning for effective recovery, particularly given the current emphasis on building in robustness for protection—an approach that may not be practical or financially affordable when addressing extreme risks (MacDonald, 2022). Take the New York City subway system as a case in point, which is prone to various flood risks from extreme rainfall, storms, and sea level rise. The system was hit by Superstorm Sandy in 2012, resulting in unprecedented destruction and sustaining $5 billion in damage (Metropolitan Transportation Authority, 2024). Despite a subsequent investment of $7.6 billion in repairs and coastal surge protections, including elevating critical infrastructure and securing subway entrances, the system was severely affected again by Tropical Storm Ida in 2021, with 75

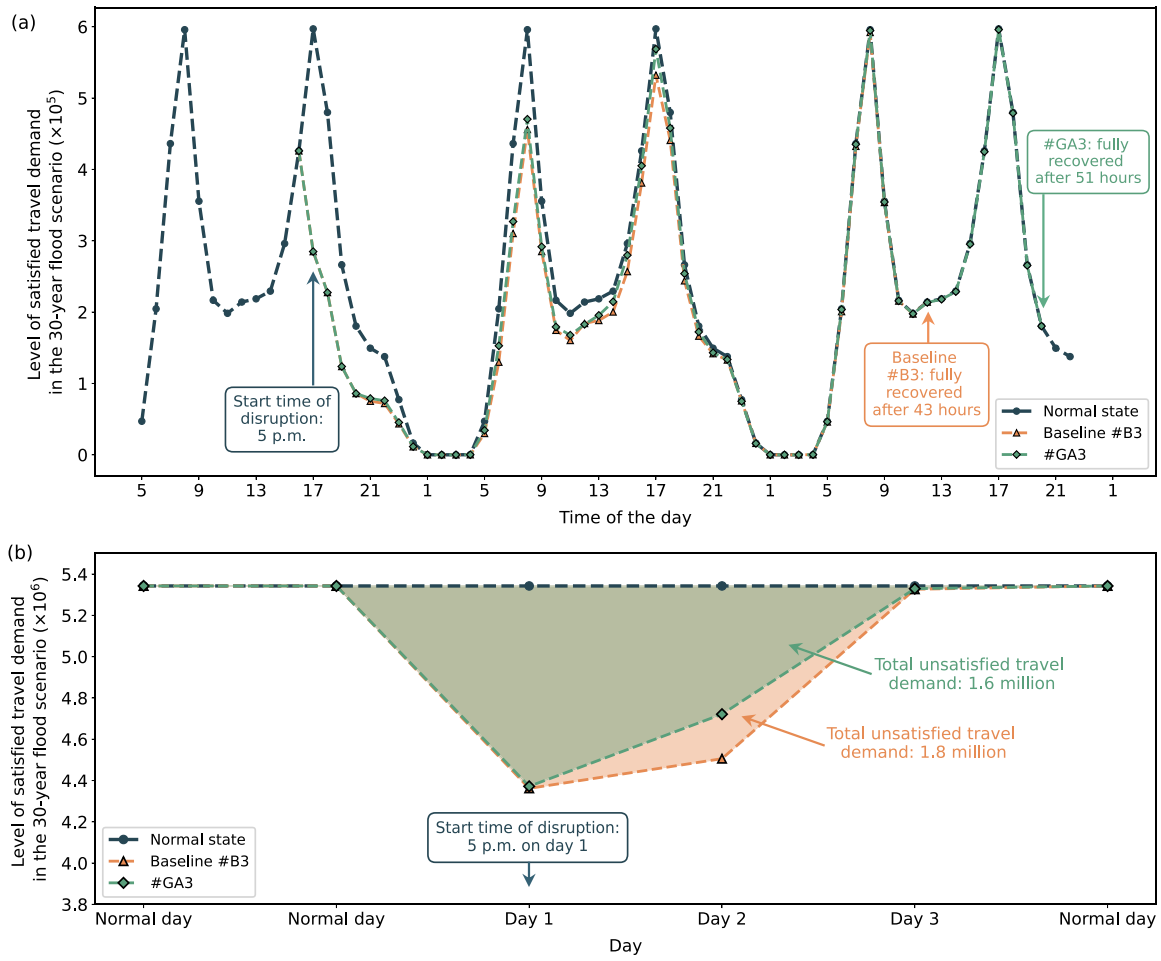

Fig. 12. Level of (a) hourly and (b) daily satisfied travel demand in the 30-year flood scenario.

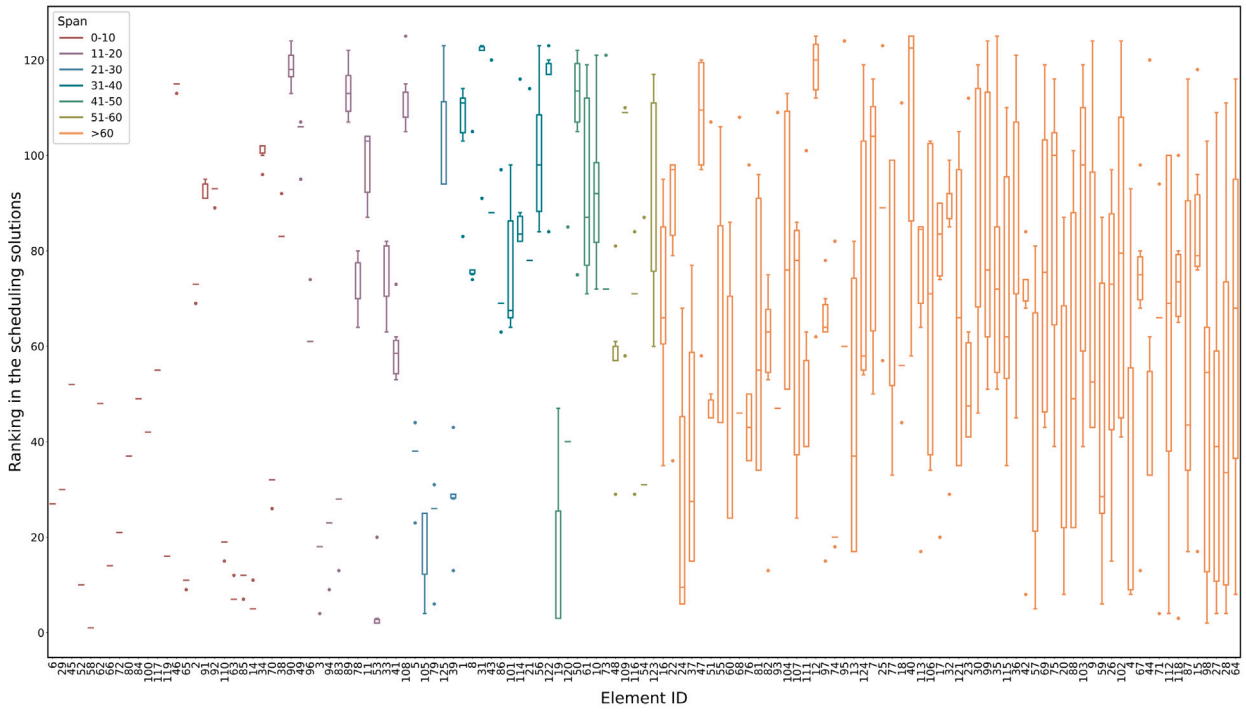

Fig. 13. A boxplot of the sequence position of each element among the six GA solutions in the 30-year flood scenario. The colours indicate the span of the positions, i.e., the difference between the most earliest and most latest positions of each element.

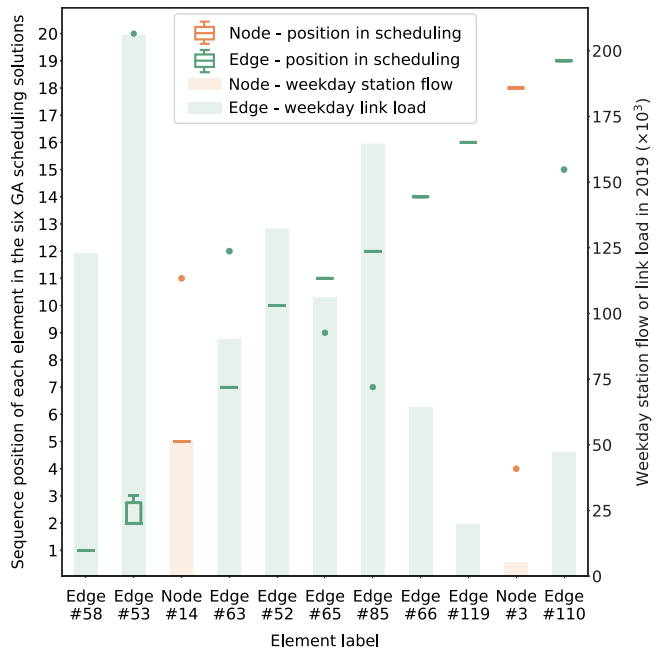

Fig. 14. Elements consistently in the top 20 positions in the 30-year flood scenario.

million gallons of water flooding it, 17 trains trapped, and damages reaching $75 million (Matthew, 2021), and by Tropical Storm Ophelia in 2023, with multiple routes completely or partially suspended (Ley, 2023). This real-world example indicates that while applying additional protection to assets is fundamental for managing recurrent and credible risks, it does not offer a complete solution against extreme but plausible threats. Moreover, as the adverse impacts of climate change will continue to intensify until at least mid-century (IPCC, 2023a), it is challenging to justify that the investment would provide satisfactory protection against impacts of all levels of magnitude in the uncertain future.

Resilience, on the other hand, highlights the transition towards safe-to-fail through prompt recovery and adaptation (Linkov et al., 2014). The case study results underscore the value of optimising critical resource scheduling for effective and efficient recovery, especially in the face of increasingly extreme flood events that could cause large-scale disruptions. Although London has not yet experienced these levels of disruption due to flooding, this does not mean that widespread disruptions are beyond the realm of possibility: the widespread floods across European in July 2021 and recently in September 2024 (Durbin, 2024) sent early warnings. This system-level approach, facilitated by network modelling and optimisation methods, helps to understand complex system dynamics during recovery. Moreover, this strategy mainly involves human and equipment costs, unlike robustness-centric strategies that necessitate extensive construction efforts, which may be less sustainable due to additional carbon costs. Therefore, achieving effective recovery presents a potentially cost-effective resilience strategy for managing disaster risk and mitigating post-hazard impacts.

6.2. Effective recovery: beyond merely a question of time

Some studies employ total recovery time to indicate recovery efficiency (Aquino et al., 2021; Bi et al., 2022; Kong et al., 2019; Vugrin et al., 2010; Zhang, Li, & Zhang, 2023; Zhang et al., 2017). While this approach is understandable, it is important to acknowledge that effective recovery is not merely a question of time, as evidenced by the findings from the London URTS case study. Although some optimised solutions require a few hours longer to complete the restoration than the baseline solution, they offer better results in terms of mitigating post-flood adverse impacts. These solutions prioritise resources to restore the most functionally critical elements, thereby quickly reinstating more service and minimising potential additional impacts caused by lags in their recovery. Therefore, it is worth noting that effective recovery is to restore as much service – or, in general, system functionality – as early as possible.

6.3. Feasibility of GAs in practical decision-making

Although the optimisation results are satisfactory, the feasibility of applying GAs in real-time decision-making on recovery resource scheduling is worth further discussion. As GAs rely on relatively stochastic processes for selection, crossover, and mutation to evolve towards better scheduling solutions over generations, the inherent randomness offers not only benefits but also challenges. As indicated in Fig. 11, the six simulations in each scenario end up with different levels of optimisation. In practice, where the computation capacity is often limited to accommodate running multiple simulations concurrently, it would be hard to guarantee the optimality of the obtained solution.

Another challenge lies in the efficient implementation of the GA-based decision model. As the scale of flood disruptions expands, the required computation time grows substantially. For instance, in the London case study, the average computational times for the respective scenarios are 53 h, 139 h, and 218 h. This greatly affects the suitability of GAs for real-time decision-making in resource scheduling optimisation. Nevertheless, the computations for the London case study serve as a proof of concept, implemented using Python and performed on a Windows desktop with below-average computing performance (with Intel Core i7-12700 processor and 32 GB of RAM). Leveraging devices with higher computing power, utilising compiled languages such as C++, and implementing parallel computing could significantly enhance computational performance.

Furthermore, this GA-based approach is context sensitive. The applicability of scheduling solutions derived from simulating hypothetical disruption scenarios as direct references for dealing with future disruptions may be constrained. Each real-world flood scenario would necessitate rerunning the model to get the specific results. This limitation arises because the gene space of the scheduling solution changes depending on the specific elements affected by flooding, and the system dynamics could vary considerably. Notwithstanding this, the pre-event scenario simulations, such as the ones presented in this research, offer a viable approach to exploring possibilities and building up capacity to scenario-test how to recover effectively. Transit agencies can obtain rainfall event data from the Met Office to simulate a series of flooding disruptions, identify vulnerable elements in the network, and evaluate their criticality under different recovery scenarios. This contributes to a proactive approach, enabling agencies to devise strategic responses and enhance resilience against future flood events.

6.4. Limitations and future work

Despite the contributions of this research, several limitations should be noted. Firstly, while this study integrates network model and OD travel flow data to estimate the satisfaction of travel demand under disruptions (i.e., whether each journey can be completed), it simplifies certain detailed operational features such as real-time train scheduling, line capacity, and queuing delay. As a result, the current estimates of losses may present a more optimistic scenario—actual losses could be higher. However, this limitation is unlikely to affect the general conclusions regarding the effectiveness of resource scheduling optimisation. This trade-off is necessary to maintain focus on delivering a holistic analysis of system-wide dynamic recovery processes and optimisation, which already incorporates a significant level of system complexity and dynamics. Future work could integrate advanced rail transit traffic models to enhance the precision of the findings.

In addition, although the network modelling in this study incorporates traffic redistribution through allowing rerouting and mode switching across rail transit services, it did not consider the temporal adjustments of passenger journeys under real-world flood disruptions. For instance, passengers unable to complete their journeys at their original planned time may select alternative times to travel during periods of partial network recovery. Such behavioural adaptations could lead to a slight overestimation of both total unsatisfied demand and consequent revenue loss. While this limitation exists, it does not materially compromise the core findings on the effectiveness of resource scheduling optimisation. Future research could undertake a dedicated study to examine behavioural changes and adaptations among passengers during flood-induced URTS service disruptions, utilising survey data to parameterise a network model or an agent-based model for improved resilience assessment and enhancement.

Moreover, while the level of satisfied travel demand is sufficient for indicating the core operational performance under extreme scenarios and can further analyse revenue loss to capture the valuable direct economic impact, the broad socio-economic consequences of service disruptions are not examined in this study. Specifically, extreme weather events such as flooding can disproportionately affect vulnerable populations, as these groups often have less access to alternative transport modes due to income and health inequalities (Transport for London, 2024). Future work should integrate this consideration into URTS flood resilience enhancement objectives, ensuring vulnerable populations' needs are prioritised in recovery strategies.

Finally, as reviewed in Section 2, recent advancements in reinforcement learning have shown the potential for optimising recovery resource scheduling for infrastructure systems, although the disruption scales in several case studies are relatively small compared to extreme scenarios. The advantages of this approach not only stem from achieving superior scheduling solutions compared to those obtained using heuristic algorithms or importance indicators but also from the feasibility of implementing the pre-trained neural network model to optimise decisions in real-time. Although reinforcement learning presents challenges in tuning a wide range of hyperparameters and achieving stable training performance when the system dynamic is complex, its optimisation effectiveness and feasibility for real-time decision-making warrant future effort.

7. Conclusions

Strategic scheduling of critical resources is essential for enhancing post-hazard recovery efficiency and boosting the resilience of infrastructure systems against extreme weather events, particularly in the face of ongoing climate change. This study investigates the effectiveness of optimising recovery resource scheduling in reducing adverse impacts of flood disruptions on URTS operations, including revenue loss and unsatisfied travel demand. To achieve this, it incorporates a GA into a URTS flood resilience assessment model, which systematically considers URTS network topology, flood disruption scenarios, and recovery profiles to simulate dynamic service delivery during the recovery process.

This novel application of GA is demonstrated by examining the impacts of surface water flood risks with return periods of 30, 100, and 1,000 years on the complex, real-world London URTS, which consists of 15 lines and served over five million daily travel demand in a normal state in 2019. Compared to the baseline solution determined by a demand-weighted betweenness centrality, the optimised resource scheduling solutions derived from the GA-based decision optimisation model have a tangible effect in reducing post-flood impacts. In this case study, revenue loss can be reduced by 10.9%, 10.7%, and 6.7% across the respective flood scenarios, corresponding to savings of approximately £337K, £708K, and £760K, along with decreased unmet travel demand of 197K, 404K, and 470K. The results highlight the noticable value of effective recovery in disaster risk management, especially in the context of extreme weather scenarios.

That said, the feasibility of using GAs for real-time decision-making in recovery resource scheduling is constrained by increased computation times as the scale of flood disruption grows under extreme scenarios. To address this limitation, it is promising for future research to integrate deep neural networks with reinforcement learning to pre-train agents for making real-time decisions on recovery resource scheduling. Outlining details of model settings in the context of enhancing URTS flood resilience will provide a worthwhile reference for applications of artificial intelligence in disaster risk management. The findings of this study have established a benchmark for assessing the optimisation performance of future reinforcement learning methods.

CRediT authorship contribution statement

Wei Bi: Writing – review & editing, Writing – original draft, Visualization, Software, Methodology, Formal analysis, Data curation, Conceptualization. **Jürgen Hackl:** Writing – review & editing, Supervision. **Kristen MacAskill:** Writing – review & editing, Supervision.

Funding

This research did not receive any specific grant from funding agencies in the public, commercial, or not-for-profit sectors.

Declaration of competing interest

The authors declare that they have no known competing financial interests or personal relationships that could have appeared to influence the work reported in this paper.

Acknowledgements

The authors are grateful to professionals from Transport for London (TfL) for their insightful feedback on the fundamental assumptions in this study. The opinions expressed in this paper are those of the authors and do not represent TfL. In addition, the first author would like to express sincere gratitude to the Funds for Women Graduates (FfWG) for its support with living expenses over the duration of this study.

Appendix A. Data details and sources

See Table A.1.

Appendix B. Assumptions on recovery times of flooded elements

See Table B.1.

Data availability

With the exception of Transport for London's internal documents, the data supporting the findings of this study can be obtained from the corresponding author upon a reasonable request.

Table A.1
Data details and sources.

Data	Details	Purposes	Sources
Geographical location	The London URTS shapefiles, including station entrances, tracks within stations, and tracks between stations	Identify flooded URTS elements	Self-drawn based on necessary information from TfL and OpenStreetMap
Engineering features	Network topology	Develop URTS network model	London Tube map from (Transport for London, 2023i)
	Types of stations and tracks	Identify flooded URTS elements	Google Street View
Operational features	Operational routes	Define partial line suspension when an edge is flooded	Route information from (Transport for London, 2022)
	Travel time between two adjacent stations (station dwell time is included)	Serve as edge weights in the network model for calculating journey time	TfL timetables (Transport for London, 2023b,2023d,2023e,2023g)
	Average station transfer time	Serve as a node attribute in the network model for calculating journey time	Provided by TfL in an online enquiry (Transport for London, 2011)
	The level of hourly travel demand between any pair of stations on a typical weekday	Serve as system performance indicator	A public NUMBAT dataset provided by Transport for London (2020)
	Historical flood incident records	Estimate recovery time	Internal data from TfL
	Single fares between any pair of stations	Estimate revenue loss	Data is extracted by TfL, but can be accessed via single fare finder of Transport for London (2023f)
Flood depth maps	Shapefiles for flood depth maps of 30-year, 100-year, and 1,000-year floods	Identify flooded URTS elements	Surface water flood risk maps developed by Environment Agency (Department of Environment Food & Rural Affairs, 2021)

Table B.1
Recovery time of flooded elements (Bi et al., 2024).

Element type	Flood location	Flood depth (m)	Recovery time (h)		
			Cleaned by an emergency crew with pumps t_p	Manually cleaned by staff at stations t_m	Naturally recede t_n
Node	Flooding at station concourse and/or at-grade tracks within stations	0.3–0.6	3	6	– (manually cleared)
		0.6–0.9	9	–	22
		0.9–1.2	15	–	36
		>1.2	20	–	48
	Flooding at concourse and underground tracks within stations	0.6–0.9	14	– (pump only)	– (pump only)
		0.9–1.2	22	– (pump only)	– (pump only)
		>1.2	30	– (pump only)	– (pump only)
Edge	Flooding at at-grade tracks between stations at the open section	0.3–0.6	3	6	– (manually cleared)
		0.6–0.9	9	–	22
		0.9–1.2	15	–	36
		>1.2	20	–	48
	Flooding at underground tracks between stations at the tunnel section	0.3–0.6	2[a]	– (pump only)	– (pump only)
		0.6–0.9	5[a]	– (pump only)	– (pump only)
		0.9–1.2	7[a]	– (pump only)	– (pump only)
		>1.2	10[a]	– (pump only)	– (pump only)

[a] These are additional times for tunnel flooding recovery to be added to the recovery time of the track between stations at the open section. For example, if the track between stations has open-section flooding with a depth of 0.9-1.2 m and tunnel-section flooding with a depth of 0.6-0.9 m, the total recovery time with the use of pumps is 15h+5h=20h.

References

Almoghathawi, Y., Barker, K., & Albert, L. A. (2019). Resilience-driven restoration model for interdependent infrastructure networks. *Reliability Engineering & System Safety*, *185*, 12–23. http://dx.doi.org/10.1016/j.ress.2018.12.006.

Almoghathawi, Y., González, A. D., & Barker, K. (2021). Exploring recovery strategies for optimal interdependent infrastructure network resilience. *Networks and Spatial Economics*, *21*(1), 229–260, https://link.springer.com/10.1007/s11067-020-09515-4.

Aquino, J. K., De Jesus, R., Garciano, L. E., Tanhueco, R., & Garciano, A. (2021). Repair sequence and recovery time in water distribution network resiliency. *GEOMATE Journal*, *20*(77), 77–83. http://dx.doi.org/10.21660/2020.77.9208.

Arab, A., Khodaei, A., Han, Z., & Khator, S. K. (2015). Proactive recovery of electric power assets for resiliency enhancement. *IEEE Access*, *3*, 99–109. http://dx.doi.org/10.1109/ACCESS.2015.2404215.

Arjomandi-Nezhad, A., Fotuhi-Firuzabad, M., Moeini-Aghtaie, M., Safdarian, A., Dehghanian, P., & Wang, F. (2020). Modeling and optimizing recovery strategies for power distribution system resilience. *IEEE Systems Journal*, *15*(4), 4725–4734. http://dx.doi.org/10.1109/JSYST.2020.3020058.

Assad, A., Moselhi, O., & Zayed, T. (2020). Resilience-driven multiobjective restoration planning for water distribution networks. *Journal of Performance of Constructed Facilities*, *34*(4), Article 04020072. http://dx.doi.org/10.1061/(ASCE)CF.1943-5509.0001478.

Aziz, T., Waseem, M., Liu, S., Ma, Y., & Lin, Z. (2023). A self-healing restoration of power grid based on two-stage adaptive decision-making strategy to enhance grid resilience. *International Journal of Electrical Power & Energy Systems*, *154*, Article 109435. http://dx.doi.org/10.1016/j.ijepes.2023.109435.

Beyza, J., Bravo, V. M., Garcia-Paricio, E., Yusta, J. M., & Artal-Sevil, J. S. (2020). Vulnerability and resilience assessment of power systems: From deterioration to recovery via a topological model based on graph theory. In *2020 IEEE international autumn meeting on power, electronics and computing: vol. 4*, (pp. 1–6). IEEE, http://dx.doi.org/10.1109/ROPEC50909.2020.9258709.

Bi, W., MacAskill, K., & Schooling, J. (2023). Old wine in new bottles? Understanding infrastructure resilience: Foundations, assessment, and limitations. *Transportation Research Part D: Transport and Environment*, *120*, Article 103793. http://dx.doi.org/10.1016/j.trd.2023.103793.

Bi, W., Schooling, J., & MacAskill, K. (2024). Assessing flood resilience of urban rail transit systems: Complex network modelling and stress testing in a case study

of London. *Transportation Research Part D: Transport and Environment*, *134*, Article 104263. http://dx.doi.org/10.1016/j.trd.2024.104263.

Bi, X., Wu, J., Sun, C., & Ji, K. (2022). Resilience-based repair strategy for gas network system and water network system in urban city. *Sustainability*, *14*(6), 3344. http://dx.doi.org/10.3390/su14063344.

Boyd, E. H., Leigh, G., & Sutton, J. (2024). *London climate resilience review interim report: Technical report*, Greater London Authority, https://www.london.gov.uk. (Accessed 1 May 2024).

Browning, O. (2023). Milan metro underpass flooded during heavy downpour. The Independent. https://www.independent.co.uk/tv/news/italy-weather-milan-flooding-metro-b2439672.html. (Accessed 5 April 2024).

Bruneau, M., Chang, S. E., Eguchi, R. T., Lee, G. C., O'Rourke, T. D., Reinhorn, A. M., Shinozuka, M., Tierney, K., Wallace, W. A., & von Winterfeldt, D. (2003). A framework to quantitatively assess and enhance the seismic resilience of communities. *Earthquake Spectra*, *19*(4), 733–752. http://dx.doi.org/10.1193/1.1623497.

Cheng, Y., & Zhang, Z. (2022). A resilience-based routing planning and scheduling model for post-disaster transportation network recovery with multiple repair teams. In *2022 4th international conference on system reliability and safety engineering* (pp. 97–103). http://dx.doi.org/10.1109/SRSE56746.2022.10067487.

Department of Environment Food & Rural Affairs (2021). Defra data services platform. Available at: https://environment.data.gov.uk/rofsw. (Accessed 1 November 2021).

Du, M., Guo, W., Zhao, J., Xie, X., Wu, Y., & Wang, Y. (2023). Strategies of repair sequence for the metro in the bus feeder scenario from the resilience perspective. In *2023 IEEE international conference on systems, man, and cybernetics* (pp. 2397–2402). IEEE, http://dx.doi.org/10.1109/SMC53992.2023.10394454.

Durbin, A. (2024). Storm boris: Italy braces for rain as 21 killed in Europe floods. BBC News. https://www.bbc.com/news/articles/ckgmrnwgm7zo. (Accessed 30 September 2024).

Edib, S. N., Lin, Y., Vokkarane, V. M., Qiu, F., Yao, R., & Chen, B. (2023). Cyber restoration of power systems: Concept and methodology for resilient observability. *IEEE Transactions on Systems, Man, and Cybernetics: Systems*, *53*(8), 5185–5198. http://dx.doi.org/10.1109/TSMC.2023.3258412.

Endler, J. A. (1986). *Natural selection in the wild*. Princeton University Press.

Fan, X., Zhang, X., Wang, X., & Yu, X. (2023). A deep reinforcement learning model for resilient road network recovery under earthquake or flooding hazards. *Journal of Infrastructure Preservation and Resilience*, *4*(1), 8. http://dx.doi.org/10.1186/s43065-023-00072-x.

Fan, X., Zhang, X., & Yu, X. (2022). A graph convolution network-deep reinforcement learning model for resilient water distribution network repair decisions. *Computer-Aided Civil and Infrastructure Engineering*, *37*(12), 1547–1565. http://dx.doi.org/10.1111/mice.12813.

Fang, Y. P., & Sansavini, G. (2019). Optimum post-disruption restoration under uncertainty for enhancing critical infrastructure resilience. *Reliability Engineering & System Safety*, *185*, 1–11. http://dx.doi.org/10.1016/j.ress.2018.12.002.

Figueroa-Candia, M., Felder, F. A., & Coit, D. W. (2018). Resiliency-based optimization of restoration policies for electric power distribution systems. *Electric Power Systems Research*, *161*, 188–198. http://dx.doi.org/10.1016/j.epsr.2018.04.007.

Gan, N., & Wang, Z. (2021). Death toll rises as passengers recount horror of China subway floods. CNN. https://www.cnn.com/2021/07/22/china/zhengzhou-henan-china-flooding-update-intl-hnk/index.html. (Accessed 17 December 2021).

Goldbeck, N., Angeloudis, P., & Ochieng, W. Y. (2019). Resilience assessment for interdependent urban infrastructure systems using dynamic network flow models. *Reliability Engineering & System Safety*, *188*, 62–79. http://dx.doi.org/10.1016/j.ress.2019.03.007.

Greater London Authority (2018). *London regional flood risk appraisal: Technical report*, https://www.london.gov.uk/sites/default/files/regional_flood_risk_appraisal_sept_2018.pdf. (Accessed 16 Feburary 2022).

Hackl, J., Adey, B. T., & Lethanh, N. (2018). Determination of near-optimal restoration programs for transportation networks following natural hazard events using simulated annealing. *Computer-Aided Civil and Infrastructure Engineering*, *33*(8), 618–637. http://dx.doi.org/10.1111/mice.12346.

Han, Z., Ma, D., Hou, B., & Wang, W. (2020). Seismic resilience enhancement of urban water distribution system using restoration priority of pipeline damages. *Sustainability*, *12*(3), 914. http://dx.doi.org/10.3390/su12030914.

Henry, E., Furno, A., & El Faouzi, N. E. (2021). REINFORCE: Rapid augmentation of large-scale multi-modal transport networks for resilience enhancement. *Applied Network Science*, *6*, 1–24. http://dx.doi.org/10.1007/s41109-021-00422-2.

Hu, J., Yang, M., & Zhen, Y. (2024). A review of resilience assessment and recovery strategies of urban rail transit networks. *Sustainability*, *16*(15), 6390. http://dx.doi.org/10.3390/su16156390.

IPCC (2023a). Summary for policymakers. In *Climate change 2023: Synthesis report. contribution of working groups I, II and III to the sixth assessment report of the intergovernmental panel on climate change* (pp. 1–34). Geneva, Switzerland: Intergovernmental Panel on Climate Change, http://dx.doi.org/10.59327/IPCC/AR6-9789291691647.001, (Accessed 6 April 2024).

IPCC (2023b). Weather and climate extreme events in a changing climate. In *Climate change 2021 – the physical science basis: Working group i contribution to the sixth assessment report of the intergovernmental panel on climate change* (pp. 1513–1766). Cambridge: Cambridge University Press.

Itani, A., & Shalaby, A. (2021). Assessing the bus bridging effectiveness on the operational resilience of the subway service in toronto. *Transportation Research Record*, *2675*(9), 1410–1422. http://dx.doi.org/10.1177/03611981211007836.

JBA (2021). A retrospective look at summer 2021 London flash floods. *JBA Risk Management*, https://www.jbarisk.com/products-services/event-response/a-retrospective-look-at-summer-2021-london-flash-floods/. (Accessed 5 April 2024).

Jin, J. G., Tang, L. C., Sun, L., & Lee, D. H. (2014). Enhancing metro network resilience via localized integration with bus services. *Transportation Research Part E: Logistics and Transportation Review*, *63*, 17–30. http://dx.doi.org/10.1016/j.tre.2014.01.002.

Jin, J. G., Teo, K. M., & Odoni, A. R. (2016). Optimizing bus bridging services in response to disruptions of urban transit rail networks. *Transportation Science*, *50*(3), 790–804. http://dx.doi.org/10.1287/trsc.2014.0577.

Karakoc, D. B., Almoghathawi, Y., Barker, K., González, A. D., & Mohebbi, S. (2019). Community resilience-driven restoration model for interdependent infrastructure networks. *International Journal of Disaster Risk Reduction*, *38*, Article 101228. http://dx.doi.org/10.1016/j.ijdrr.2019.101228.

Kong, J., Zhang, C., & Simonovic, S. P. (2019). A two-stage restoration resource allocation model for enhancing the resilience of interdependent infrastructure systems. *Sustainability*, *11*(19), 5143. http://dx.doi.org/10.3390/su11195143.

Kong, J., Zhang, C., & Simonovic, S. P. (2023). Resilience and risk-based restoration strategies for critical infrastructure under uncertain disaster scenarios. *Sustainable Cities and Society*, *92*, Article 104510. http://dx.doi.org/10.1016/j.scs.2023.104510.

Lambora, A., Gupta, K., & Chopra, K. (2019). Genetic algorithm- a literature review. In *2019 international conference on machine learning, big data, cloud and parallel computing* (pp. 380–384). http://dx.doi.org/10.1109/COMITCon.2019.8862255.

Lei, S., Chen, C., Li, Y., & Hou, Y. (2019). Resilient disaster recovery logistics of distribution systems: Co-optimize service restoration with repair crew and mobile power source dispatch. *IEEE Transactions on Smart Grid*, *10*(6), 6187–6202. http://dx.doi.org/10.1109/TSG.2019.2899353.

Ley, A. (2023). Rain wreaks havoc on new york's mass transit system. The New York Times. https://www.nytimes.com/2023/09/29/nyregion/nyc-flood-mta-subway.html. (Accessed 24 April 2024).

Li, W., Mazumder, R. K., & Li, Y. (2023). Topology-based resilience metrics for seismic performance evaluation and recovery analysis of water distribution systems. *Journal of Pipeline Systems Engineering and Practice*, *14*(1), Article 04022070. http://dx.doi.org/10.1061/JPSEA2.PSENG-1303.

Li, Z., Shahidehpour, M., Galvin, R. W., & Li, Y. (2018). Collaborative cyber-physical restoration for enhancing the resilience of power distribution systems. In *2018 IEEE power & energy society general meeting* (pp. 1–5). IEEE, http://dx.doi.org/10.1109/PESGM.2018.8585955.

Li, J., Xu, Y., Wang, Y., Li, M., He, J., Liu, C. C., & Schneider, K. P. (2021). Resilience-motivated distribution system restoration considering electricity-water-gas interdependency. *IEEE Transactions on Smart Grid*, *12*(6), 4799–4812. http://dx.doi.org/10.1109/TSG.2021.3105234.

Linder, L. (2022). Genetic algorithms with PyGAD: Selection, crossover, mutation. DERLIN. https://blog.derlin.ch/genetic-algorithms-with-pygad. (Accessed 30 September 2023).

Linkov, I., Bridges, T., Creutzig, F., Decker, J., Fox-Lent, C., Kröger, W., Lambert, J. H., Levermann, A., Montreuil, B., Nathwani, J., Nyer, R., Renn, O., Scharte, B., Scheffler, A., Schreurs, M., & Thiel-Clemen, T. (2014). Changing the resilience paradigm. *Nature Climate Change*, *4*(6), 407–409. http://dx.doi.org/10.1038/nclimate2227.

Liu, Z., Chen, H., Liu, E., & Zhang, Q. (2022). Evaluating the dynamic resilience of the multi-mode public transit network for sustainable transport. *Journal of Cleaner Production*, *348*, Article 131350. http://dx.doi.org/10.1016/j.jclepro.2022.131350.

Liu, Y., McNeil, S., Hackl, J., & Adey, B. T. (2022). Prioritizing transportation network recovery using a resilience measure. *Sustainable and Resilient Infrastructure*, *7*(1), 70–81. http://dx.doi.org/10.1080/23789689.2019.1708180.

Liu, W., Song, Z., Ouyang, M., & Li, J. (2020). Recovery-based seismic resilience enhancement strategies of water distribution networks. *Reliability Engineering & System Safety*, *203*, Article 107088. http://dx.doi.org/10.1016/j.ress.2020.107088.

Liu, Z., Sun, D. J., Chen, H., Hao, W., Wang, Z., & Tang, F. (2024). Resilience-based post-disaster repair strategy for integrated public transit networks. *Transportmetrica B: Transport Dynamics*, *12*(1), 1–25. http://dx.doi.org/10.1080/21680566.2024.2352494.

Liu, K., Zhai, C., & Dong, Y. (2021). Optimal restoration schedules of transportation network considering resilience. *Structure and Infrastructure Engineering*, *17*(8), 1141–1154. http://dx.doi.org/10.1080/15732479.2020.1801764.

Luo, Z., & Yang, B. (2021). Towards resilient and smart urban road networks: Connectivity restoration via community structure. *Sustainable Cities and Society*, *75*, Article 103344. http://dx.doi.org/10.1016/j.scs.2021.103344.

Ma, Z., Yang, X., Wu, J. J., Chen, A. T. Y., Wei, Y., & Gao, Z. Y. (2022). Measuring the resilience of an urban rail transit network: A multi-dimensional evaluation model. *Transport Policy*, *129*, 38–50. http://dx.doi.org/10.1016/j.tranpol.2022.10.003.

MacDonald, M. (2022). *London flooding review stage 3: Performance of schemes and hotspot areas: Technical report*, https://londonfloodreview.co.uk/stage-3-report/. (Accessed 16 December 2022).

Mao, X., Zhou, J., Yuan, C., & Liu, D. (2021). Resilience-based optimization of post-disaster restoration strategy for road networks. *Journal of Advanced Transportation*, *2021*, Article e8871876. http://dx.doi.org/10.1155/2021/8871876.

Martello, M. V., Whittle, A. J., & Lyons-Galante, H. R. (2023). Depth-damage curves for rail rapid transit infrastructure. *Journal of Flood Risk Management*, *16*(1), Article e12856. http://dx.doi.org/10.1111/jfr3.12856.

Martello, M., Whittle, A. J., Keenan, J. M., & Salvucci, F. P. (2021). Evaluation of climate change resilience for Boston's rail rapid transit network. *Transportation Research Part D: Transport and Environment*, *97*, Article 102908. http://dx.doi.org/10.1016/j.trd.2021.102908.

Maryland Transit Administration (2023). Adaptation & resiliency toolbox. Available at: https://www.resilientmdotmta.com. (Accessed 9 May 2024).

Matthew, I. (2021). Ida sent 75 million gallons of water into NY subway system, caused $75M in damages. Newsweek. https://www.newsweek.com/ida-sent-75-million-gallons-water-ny-subway-system-caused-75m-damages-1629826. (Accessed 22 April 2022).

Merschman, E., Doustmohammadi, M., Salman, A. M., & Anderson, M. (2020). Postdisaster decision framework for bridge repair prioritization to improve road network resilience. *Transportation Research Record*, *2674*(3), 81–92. http://dx.doi.org/10.1177/0361198120908870.

Metropolitan Transportation Authority (2024). *Climate resilience roadmap*: *Technical report*, https://new.mta.info/document/136871. (Accessed 30 April 2024).

Mitchell, M. (1998). *An introduction to genetic algorithms*. Cambridge, Massachusetts: MIT Press, http://dx.doi.org/10.7551/mitpress/3927.001.0001.

Moghtadernejad, S., Adey, B. T., & Hackl, J. (2022). Prioritizing road network restorative interventions using a discrete particle swarm optimization. *Journal of Infrastructure Systems*, *28*(4), Article 04022039. http://dx.doi.org/10.1061/(ASCE)IS.1943-555X.0000725.

Mok, D., Kong, H., & Tsang, D. (2023). 132 hongkongers sent to hospitals, all rainstorm alerts cancelled after deluge. South China Morning Post. https://www.scmp.com/news/hong-kong/health-environment/article/3233782/hong-kong-observatory-issues-red-rainstorm-alert-warns-significant-road-flooding. (Accessed 24 April 2024).

Ouyang, M., Liu, C., & Xu, M. (2019). Value of resilience-based solutions on critical infrastructure protection: Comparing with robustness-based solutions. *Reliability Engineering & System Safety*, *190*, Article 106506. http://dx.doi.org/10.1016/j.ress.2019.106506, Publisher: Elsevier.

Pan, X., Dang, Y., Wang, H., Hong, D., Li, Y., & Deng, H. (2022). Resilience model and recovery strategy of transportation network based on travel OD-grid analysis. *Reliability Engineering & System Safety*, *223*, Article 108483. http://dx.doi.org/10.1016/j.ress.2022.108483.

Pei, S., Zhai, C., & Hu, J. (2024). Surrogate model-assisted seismic resilience assessment of the interdependent transportation and healthcare system considering a two-stage recovery strategy. *Reliability Engineering & System Safety*, *244*, Article 109941. http://dx.doi.org/10.1016/j.ress.2024.109941.

Reyes, R. (2023). Moment madrid commuters are caught in flooded metro. New York Post. https://nypost.com/2023/09/04/moment-madrid-commuters-are-caught-in-flooded-metro/. (Accessed 5 April 2024).

Saadat, Y., Ayyub, B. M., Zhang, Y., Zhang, D., & Huang, H. (2020). Resilience-based strategies for topology enhancement and recovery of metrorail transit networks. *ASCE-ASME Journal of Risk and Uncertainty in Engineering Systems, Part A: Civil Engineering*, *6*(2), Article 04020017. http://dx.doi.org/10.1061/AJRUA6.0001057.

Sadnan, R., Poudel, S., Dubey, A., & Schneider, K. P. (2022). Layered coordination architecture for resilient restoration of power distribution systems. *IEEE Transactions on Industrial Informatics*, *19*(4), 6069–6080. http://dx.doi.org/10.1109/TII.2022.3177464.

Sang, M., Ding, Y., Bao, M., Li, S., Ye, C., & Fang, Y. (2021). Resilience-based restoration strategy optimization for interdependent gas and power networks. *Applied Energy*, *302*, Article 117560. http://dx.doi.org/10.1016/j.apenergy.2021.117560.

Serdar, M. Z., & Al-Ghamdi, S. G. (2023). Resilience-oriented recovery of flooded road networks during mega-sport events: A novel framework. *Frontiers in Built Environment*, *9*, Article 1216919. http://dx.doi.org/10.3389/fbuil.2023.1216919.

Serdar, M. Z., Koc, M., & Al-Ghamdi, S. G. (2022). Urban transportation networks resilience: Indicators, disturbances, and assessment methods. *Sustainable Cities and Society*, *76*, Article 103452. http://dx.doi.org/10.1016/j.scs.2021.103452.

Somy, S., Shafaei, R., & Ramezanian, R. (2022). Resilience-based mathematical model to restore disrupted road-bridge transportation networks. *Structure and Infrastructure Engineering*, *18*(9), 1334–1349. http://dx.doi.org/10.1080/15732479.2021.1906711.

Song, Z., Liu, W., & Shu, S. (2022). Resilience-based post-earthquake recovery optimization of water distribution networks. *International Journal of Disaster Risk Reduction*, *74*, Article 102934. http://dx.doi.org/10.1016/j.ijdrr.2022.102934.

Spearman, C. (1961). The proof and measurement of association between two things. In *Studies in individual differences: The search for intelligence*, (p. 58). East Norwalk, CT, US: Appleton-Century-Crofts, https://psycnet.apa.org/doi/10.1037/11491-005.

Sutton, R. S., & Barto, A. G. (2018). *Reinforcement learning: An introduction*. Cambridge, Massachusetts: MIT Press.

The White House (2013). PPD-21: The presidential policy directive on critical infrastructure security and resilience. Whitehouse.Gov. Available at: https://obamawhitehouse.archives.gov/the-press-office/2013/02/12/presidential-policy-directive-critical-infrastructure-security-and-resil. (Accessed 14 March 2022).

Transport for London (2011). Gate-to-platform and interchange walking times - a freedom of information request to transport for London. WhatDoTheyKnow. Available at: https://www.whatdotheyknow.com/request/gate_to_platform_and_interchange. (Accessed 31 January 2024).

Transport for London (2020). TfL crowding data. Available at: http://crowding.data.tfl.gov.uk/. (Accessed 19 April 2022).

Transport for London (2022). Travel information - stations, stops & piers. Available at: https://www.tfl.gov.uk/travel-information/stations-stops-and-piers/. (Accessed 2 May 2022).

Transport for London (2023a). *Climate change adaptation plan 2023*: *Technical report*, https://content.tfl.gov.uk/tfl-climate-change-adaptation-plan.pdf. (Accessed 30 May 2023).

Transport for London (2023b). Elizabeth line timetables. Available at: https://www.tfl.gov.uk/modes/elizabeth-line/elizabeth-line-timetables. (Accessed 11 April 2023).

Transport for London (2023c). London overground and elizabeth line delays. Available at: https://www.tfl.gov.uk/fares/refunds-and-replacements/overground-and-elizabeth-line-delays. (Accessed 16 March 2023).

Transport for London (2023d). London overground timetables. Available at: https://www.tfl.gov.uk/modes/london-overground/london-overground-timetables. [Accessed 11 April 2023].

Transport for London (2023e). London underground timetables. Available at: https://www.tfl.gov.uk/modes/tube/first-and-last-tube. (Accessed 11 April 2023).

Transport for London (2023f). Single fare finder. Available at: https://www.tfl.gov.uk/fares/find-fares/tube-and-rail-fares/single-fare-finder. (Accessed 8 June 2023).

Transport for London (2023g). Tram timetable. Available at: https://tfl.gov.uk/tram/timetable/tram. (Accessed 11 Aptil 2023).

Transport for London (2023h). Tube and DLR delays. Available at: https://www.tfl.gov.uk/fares/refunds-and-replacements/tube-and-dlr-delays. (Accessed 16 March 2023).

Transport for London (2023i). Tube and rail map. Available at: https://tfl.gov.uk/maps/track?intcmp=40400. (Accessed 8 June 2023).

Transport for London (2024a). *Equity in motion: Our journey to creating a fair, accessible and inclusive transport network*: *Technical report*, https://content.tfl.gov.uk/equity-in-motion-full.pdf. (Accessed 22 Aril 2024).

Transport for London (2024b). *Travel in London 2024: The travel behaviour of London residents based on the London travel demand survey*: *Technical report*, https://content.tfl.gov.uk/travel-in-london-2024-the-travel-behaviour-of-london-residents-based-on-the-ltds-acc.pdf. (Accessed 28 December 2024).

Transportation Research Board (2021). *Investing in transportation resilience: A framework for informed choices*: *Technical report*, Washington, DC: The National Academies Press, http://dx.doi.org/10.17226/26292, (Accessed 1 January 2025).

UK Met Office (2019). What causes flash floods? Available at: https://www.metoffice.gov.uk/weather/learn-about/weather/types-of-weather/rain/flash-floods. (Accessed 9 May 2024).

United Nations (2015). THE 17 GOALS. Available at: https://sdgs.un.org/goals. (Accessed 26 March 2024).

US NOAA (2016). *Flash flooding definition*. NOAA's National Weather Service, Available at: https://www.weather.gov/phi/FlashFloodingDefinition. (Accessed 9 May 2024).

Vugrin, E. D., Warren, D. E., Ehlen, M. A., & Camphouse, R. C. (2010). A framework for assessing the resilience of infrastructure and economic systems. In K. Gopalakrishnan, & S. Peeta (Eds.), *Sustainable and resilient critical infrastructure systems* (pp. 77–116). Berlin, Heidelberg: Springer, http://link.springer.com/10.1007/978-3-642-11405-2_3. (Accessed 16 November 2021).

Wang, Y., Qiu, D., Teng, F., & Strbac, G. (2023). Towards microgrid resilience enhancement via mobile power sources and repair crews: A multi-agent reinforcement learning approach. *IEEE Transactions on Power Systems*, *39*(1), 1329–1345. http://dx.doi.org/10.1109/TPWRS.2023.3240479.

Wang, J., Yuan, Z., & Yin, Y. (2019). Optimization of bus bridging service under unexpected metro disruptions with dynamic passenger flows. *Journal of Advanced Transportation*, *2019*(1), Article 6965728. http://dx.doi.org/10.1155/2019/6965728.

Wu, Y., Hou, G., & Chen, S. (2021). Post-earthquake resilience assessment and long-term restoration prioritization of transportation network. *Reliability Engineering & System Safety*, *211*, Article 107612. http://dx.doi.org/10.1016/j.ress.2021.107612.

Wu, G., Li, M., & Li, Z. S. (2020). Resilience-based optimal recovery strategy for cyber–physical power systems considering component multistate failures. *IEEE Transactions on Reliability*, *70*(4), 1510–1524. http://dx.doi.org/10.1109/TR.2020.3025179.

Xu, M., Li, G., & Chen, A. (2024). Resilience-driven post-disaster restoration of interdependent infrastructure systems under different decision-making environments. *Reliability Engineering & System Safety*, *241*, Article 109599. http://dx.doi.org/10.1016/j.ress.2023.109599.

Xu, P. C., Lu, Q. C., Xie, C., & Cheong, T. (2024). Modeling the resilience of interdependent networks: The role of function dependency in metro and bus systems. *Transportation Research Part A: Policy and Practice*, *179*, Article 103907. http://dx.doi.org/10.1016/j.tra.2023.103907.

Xu, C., & Xu, X. (2024). A two-stage resilience promotion approach for urban rail transit networks based on topology enhancement and recovery optimization. *Physica A. Statistical Mechanics and its Applications*, *635*, Article 129496. http://dx.doi.org/10.1016/j.physa.2024.129496.

Yadav, N., Chatterjee, S., & Ganguly, A. R. (2020). Resilience of urban transport network-of-networks under intense flood hazards exacerbated by targeted attacks. *Scientific Reports*, *10*(1), 10350. http://dx.doi.org/10.1038/s41598-020-66049-y.

Yang, W., Shanshan, F., Bing, W., Jinhui, H., & Xiaoyang, W. (2018). Towards optimal recovery scheduling for dynamic resilience of networked infrastructure. *Journal of Systems Engineering and Electronics*, *29*(5), 995–1008. http://dx.doi.org/10.21629/JSEE.2018.05.11.

Yang, S., Zhang, Y., Lu, X., Guo, W., & Miao, H. (2024). Multi-agent deep reinforcement learning based decision support model for resilient community post-hazard recovery. *Reliability Engineering & System Safety*, *242*, Article 109754. http://dx.doi.org/10.1016/j.ress.2023.109754.

Zhang, W., Han, Q., Dong, H., Wen, J., & Xu, C. (2024). Resilience-based post-earthquake restoration scheduling for urban interdependent transportation-electric power network. *Structure and Infrastructure Engineering*, 1–18. http://dx.doi.org/10.1080/15732479.2024.2347496.

Zhang, C., Kong, J. j., & Simonovic, S. P. (2018). Restoration resource allocation model for enhancing resilience of interdependent infrastructure systems. *Safety Science*, *102*, 169–177. http://dx.doi.org/10.1016/j.ssci.2017.10.014.

Zhang, J., Li, G., & Zhang, M. (2023). Multi-objective optimization for community building group recovery scheduling and resilience evaluation under earthquake. *Computer-Aided Civil and Infrastructure Engineering*, *38*(12), 1657–1676. http://dx.doi.org/10.1111/mice.12882.

Zhang, Y., & Ng, S. T. (2021). A hypothesis-driven framework for resilience analysis of public transport network under compound failure scenarios. *International Journal of Critical Infrastructure Protection*, *35*, Article 100455. http://dx.doi.org/10.1016/j.ijcip.2021.100455.

Zhang, J., Ren, G., & Song, J. (2022). Resilience-based restoration sequence optimization for metro networks: A case study in China. *Journal of Advanced Transportation*, *2022*(1), Article e8595356. http://dx.doi.org/10.1155/2022/8595356.

Zhang, J., Ren, G., & Song, J. (2023). Resilience-based optimization model for emergency bus bridging and dispatching in response to metro operational disruptions. *PLoS One*, *18*(3), Article e0277577. http://dx.doi.org/10.1371/journal.pone.0277577.

Zhang, W., Wang, N., & Nicholson, C. (2017). Resilience-based post-disaster recovery strategies for road-bridge networks. *Structure and Infrastructure Engineering*, *13*(11), 1404–1413. http://dx.doi.org/10.1080/15732479.2016.1271813.

Zheng, M., Zuo, H., Zhou, Z., & Bai, Y. (2023). Recovery strategies for urban rail transit network based on comprehensive resilience. *Sustainability*, *15*(20), 15018. http://dx.doi.org/10.3390/su152015018.

Zhu, M., Chen, J., & Yin, Y. (2021). Repair strategies of an urban rail transit network based on optimal resilience. In *2021 6th international conference on transportation information and safety* (pp. 871–876). IEEE, http://dx.doi.org/10.1109/ICTIS54573.2021.9798463.